

FRA-76-5  
REPORT NO. FRA-OR&D-76-246

## MECHANICS OF TRAIN COLLISION

Pin Tong

U.S. DEPARTMENT OF TRANSPORTATION  
Transportation Systems Center  
Kendall Square  
Cambridge MA 02142



APRIL 1976  
FINAL REPORT

DOCUMENT IS AVAILABLE TO THE PUBLIC  
THROUGH THE NATIONAL TECHNICAL  
INFORMATION SERVICE, SPRINGFIELD,  
VIRGINIA 22161

Prepared for  
U.S. DEPARTMENT OF TRANSPORTATION  
FEDERAL RAILROAD ADMINISTRATION  
Office of Research and Development  
Washington DC 20590

NOTICE

This document is disseminated under the sponsorship of the Department of Transportation in the interest of information exchange. The United States Government assumes no liability for its contents or use thereof.

NOTICE

The United States Government does not endorse products or manufacturers. Trade or manufacturers' names appear herein solely because they are considered essential to the object of this report.

Technical Report Documentation Page

1. Report No. FRA-OR&D-76-246		2. Government Accession No.		3. Recipient's Catalog No.	
4. Title and Subtitle MECHANICS OF TRAIN COLLISION				5. Report Date April 1976	
				6. Performing Organization Code	
7. Author(s) Pin Tong				8. Performing Organization Report No. DOT-TSC-FRA-76-5	
9. Performing Organization Name and Address U.S. Department of Transportation Transportation Systems Center Kendall Square Cambridge MA 02142				10. Work Unit No. (TRAIS) RR628/R6317	
				11. Contract or Grant No.	
12. Sponsoring Agency Name and Address U.S. Department of Transportation Federal Railroad Administration Office of Research and Development Washington DC 20590				13. Type of Report and Period Covered Final Report September 1974 - March 1976	
				14. Sponsoring Agency Code	
15. Supplementary Notes					
16. Abstract  A simple and a more detailed mathematical model for the simulation of train collisions are presented. The study presents considerable insight as to the causes and consequences of train motions in impact. Comparison of model predictions with two full scale train-to-train impact tests shows good correlation. Methods for controlling train motion and kinetic energy dissipation for the minimization of train collision induced damage are suggested.					
17. Key Words Crashworthiness, Collision, Train, Locomotive, Caboose, Finite Element Solution, Mechanics				18. Distribution Statement  DOCUMENT IS AVAILABLE TO THE U.S. PUBLIC THROUGH THE NATIONAL TECHNICAL INFORMATION SERVICE, SPRINGFIELD, VIRGINIA 22161	
19. Security Classif. (of this report) Unclassified		20. Security Classif. (of this page) Unclassified		21. No. of Pages 74	22. Price



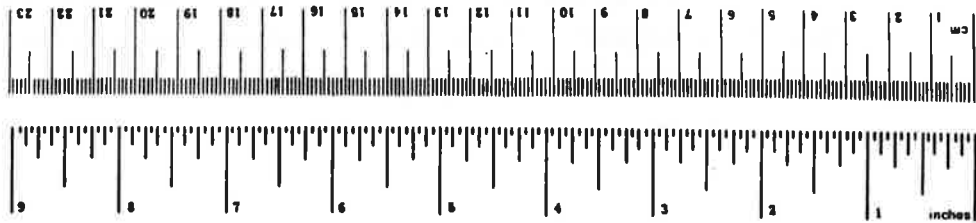
## PREFACE

Each year train accidents claim lives and account for many injuries and much property damage. Concern for the safety of the public and of the operating crews dictates the important segments of the safety research program of the Federal Railroad Administration (FRA) which are devoted to the reduction of train collision, improving crashworthiness of locomotives, cabooses and other rail vehicles, and reducing property damage. In order to achieve these goals, it is necessary to be able to control the car motion and to dissipate properly the kinetic energy in collision. But first, one must understand the mechanism of the car motion and the reasons why the impacting cars behave as they do (override, jackknife, etc.) in impact. This report summarizes the analytical study seeking such understanding.

# METRIC CONVERSION FACTORS

## Approximate Conversions to Metric Measures

Symbol	When You Know	Multiply by	To Find	Symbol
<b>LENGTH</b>				
in	inches	2.5	centimeters	cm
ft	feet	30	centimeters	cm
yd	yards	0.9	meters	m
mi	miles	1.6	kilometers	km
<b>AREA</b>				
in <sup>2</sup>	square inches	6.5	square centimeters	cm <sup>2</sup>
ft <sup>2</sup>	square feet	0.09	square meters	m <sup>2</sup>
yd <sup>2</sup>	square yards	0.8	square meters	m <sup>2</sup>
mi <sup>2</sup>	square miles	2.6	square kilometers	km <sup>2</sup>
	acres	0.4	hectares	ha
<b>MASS (weight)</b>				
oz	ounces	28	grams	g
lb	pounds	0.45	kilograms	kg
	short tons (2000 lb)	0.9	tonnes	t
<b>VOLUME</b>				
teaspoon	teaspoons	5	milliliters	ml
fl oz	fluid ounces	15	milliliters	ml
c	cups	30	milliliters	ml
pt	pints	0.24	liters	l
qt	quarts	0.47	liters	l
gal	gallons	0.95	liters	l
ft <sup>3</sup>	cubic feet	2.8	liters	l
yd <sup>3</sup>	cubic yards	0.03	cubic meters	m <sup>3</sup>
		0.76	cubic meters	m <sup>3</sup>
<b>TEMPERATURE (exact)</b>				
°F	Fahrenheit temperature	5/9 (after subtracting 32)	Celsius temperature	°C



## Approximate Conversions from Metric Measures

Symbol	When You Know	Multiply by	To Find	Symbol
<b>LENGTH</b>				
mm	millimeters	0.04	inches	in
cm	centimeters	0.4	inches	in
m	meters	3.3	feet	ft
km	kilometers	1.1	yards	yd
		0.6	miles	mi
<b>AREA</b>				
cm <sup>2</sup>	square centimeters	0.16	square inches	in <sup>2</sup>
m <sup>2</sup>	square meters	1.2	square yards	yd <sup>2</sup>
km <sup>2</sup>	square kilometers	0.4	square miles	mi <sup>2</sup>
ha	hectares (10,000 m <sup>2</sup> )	2.6	square miles	mi <sup>2</sup>
<b>MASS (weight)</b>				
g	grams	0.035	ounces	oz
kg	kilograms	2.2	pounds	lb
t	tonnes (1000 kg)	1.1	short tons	
<b>VOLUME</b>				
ml	milliliters	0.03	fluid ounces	fl oz
l	liters	2.1	pints	pt
		1.06	quarts	qt
		0.26	gallons	gal
m <sup>3</sup>	cubic meters	36	cubic feet	ft <sup>3</sup>
		1.3	cubic yards	yd <sup>3</sup>
<b>TEMPERATURE (exact)</b>				
°C	Celsius temperature	9/5 (then add 32)	Fahrenheit temperature	°F

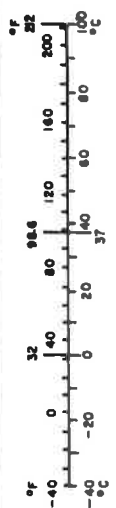


## TABLE OF CONTENTS

<u>Section</u>	<u>Page</u>
1. INTRODUCTION .....	1
2. CAR MOTION IN COLLISION .....	2
2.1 Estimation of Longitudinal Forces .....	2
2.2 Estimation of the Vertical and Pitch Motions of the Impacted Car .....	9
2.3 Effect of Misalignment.....	15
3. MECHANISM OF OVERRIDE .....	18
4. NUMERICAL SIMULATION OF REAR END COLLISION OF TRAINS .....	31
5. CONCLUSIONS, DISCUSSIONS AND RECOMMENDATIONS .....	41
APPENDIX A - LONGITUDINAL AND VERTICAL MOTION OF THREE IMPACTING MASSES .....	49
APPENDIX B - MODELING OF TRAINS BY FINITE ELEMENT MODULES .....	57
REFERENCES .....	65

## LIST OF ILLUSTRATIONS

<u>Figure</u>	<u>Page</u>
1 TRAIN COLLISION AND POSSIBLE OUTCOMES .....	3
2 COLLISION OF THREE MASSES .....	4
3 LONGITUDINAL FORCES AT BOTH ENDS .....	8
4 INDUCED VERTICAL AND PITCHING MOTION AFTER IMPACT .....	10
5 NORMALIZED VERTICAL VELOCITY AND DISPLACEMENT .....	12
6 OVERRIDE MODES VS. IMPACT SPEED FOR THE PARAMETERS GIVEN IN EQUATION 3 .....	16
7 TRANSMISSION OF LONGITUDINAL FORCES .....	20

## LIST OF ILLUSTRATIONS (CONT'D)

<u>Figure</u>		<u>Page</u>
8	CROSS-SECTION OF THE CENTER SILL AND THE COUPLER SHANK .....	21
9	FACTORS CONTRIBUTE TO OVERRIDE ON CAR 2 .....	23
10	MATHEMATICAL MODEL OF A RAIL CAR .....	32
11	DETAIL MODELING OF A CAR BODY FOR HIGH SPEED IMPACT .....	33
12	CUTS OF CARS FOR 18MPH REAR END COLLISION TEST ...	34
13	CUTS OF CARS FOR 30MPH REAR END COLLISION TEST ...	34
14	LONGITUDINAL FORCES AT BOTH ENDS OF THE CABOOSE FOR 18.1 MPH IMPACT — COMPUTER SIMULATION --- FULL SCALE TEST .....	35
15	SLIPPAGE BETWEEN THE IMPACTED CAR AND THE BACK UP CAR FOR 18.1 MPH IMPACT .....	38
16	LONGITUDINAL FORCES ON THE CABOOSE FOR A 30.3 MPH IMPACT — COMPUTER SIMULATION --- FULL SCALE TEST TEST .....	40
17	FINAL CONFIGURATION OF THE CABOOSE AFTER THE 30MPH COLLISION .....	46
18	CRASHWORTHY AND OVERRIDEWORTHY LOCOMOTIVE.....	47
19	TYPICAL SPRING CHARACTERISTICS .....	58
20	TWO IMPACTIVE COUPLERS WITH DOTTED LINES INDICATE THE DEFORMATION .....	61
21	SCHEMATIC DIAGRAM OF THE FAILURE OF APPROXIMATE SOLUTION IN ELASTIC PLASTIC ANALYSIS .....	64

## LIST OF TABLES

<u>Table</u>		<u>Page</u>
1	SUMMARY OF OVERRIDE MODES AND TRAIN CONFIGURATIONS .....	30

LIST OF TABLES (CONT'D)

<u>Table</u>		<u>Page</u>
2	PARAMETERS USED FOR TRAIN-TO-TRAIN IMPACT SIMULATION .....	36
3	MATERIAL PROPERTIES OF BEAM ELEMENTS OF CABOOSE ..	39
4	WEIGHT AND ROTARY INERTIA OF EACH NODE OF CABOOSE .....	39



## 1. INTRODUCTION

Each year train accidents claim lives and account for many injuries and much property damage.<sup>1</sup> The concern for the safety of the public and of the operating crews dictates important segments of the safety research program of the Federal Railroad Administration (FRA) devoted to the reduction of train collision and improving crashworthiness of locomotives, cabooses and other rail vehicles. Among the train accidents, tank car collisions resulting in fire and explosion, and rear end collisions resulting in override of one car on another are the most severe type. The former is particularly important in terms of public safety and to property damage, and the latter is especially important for the safety of the crews in the locomotive and in the caboose.<sup>2</sup>

The objective of the present study is to gain insight into the mechanism of car motion during train impact, and to seek effective measures of controlling kinetic energy dissipation during collisions in order to reduce casualties and damage.

The discussion in this report will focus on the mechanism of override. The comparison of analytical results with full scale rear end collision tests will be presented.

## 2. CAR MOTION IN COLLISION

Some of the possible post collision configurations as a result of train impacts are shown schematically in Figure 1. The collision may result in severe damage to the trains due to the end car (in many cases a caboose) of the impacted train jumping up and overriding the locomotive (or the front car), or crushing and/or buckling of the impacting cars, or jackknifing and derailment, etc. These events can also occur in other parts of the trains. The actual resulting situation in a given accident depends upon the impact velocity, the consist of the trains, locations of trucks, weight and mass moments of inertia of the cars and lading, stiffness and strength of various components (such as draft gear, underframe, bolster, and truck etc.), the alignment and the slack of the coupler, the friction coefficient between couplers, and the friction coefficient between wheels and rails if emergency brakes are on.

The detailed interactions between the cars and their deformation are highly complex. However, the controlling mechanism of car motion for the short time duration immediately after impact can be obtained by a simple approximation.

### 2.1 ESTIMATION OF LONGITUDINAL FORCES

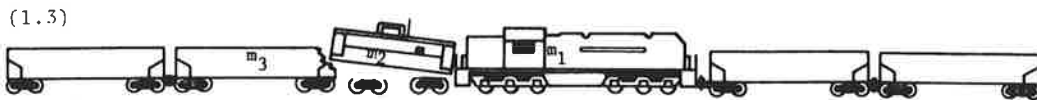
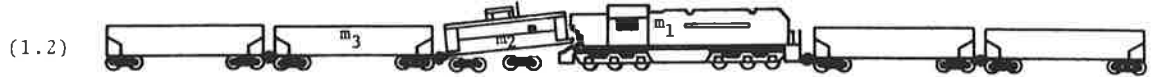
We shall first estimate the longitudinal forces at the impact end (subsequently called the A end) and at the front end, (subsequently called the B end) of the impacted car, which will be denoted by  $F_1$  and  $F_2$  respectively. The approximate model of impact is shown in Figure 2, where  $m_1$ ,  $m_2^*$  and  $m_3$  are respectively the masses of the impacting car, the impacted car and the back-up freight car;  $k_1$  and  $k_2$  are the spring constants representing the

---

\* We have to consider the mass of the impacted car body only. This is so because during impact the truck is only minimally involved initially in the horizontal motion and hence its effect is negligible.

B end

A end



(1.7) OTHERS SUCH AS JACKKNIFING, LATERAL DERAILMENT AND A SIMILAR PHENOMENON IN OTHER PART OF CONSIST

FIGURE 1. TRAIN COLLISION AND POSSIBLE OUTCOMES

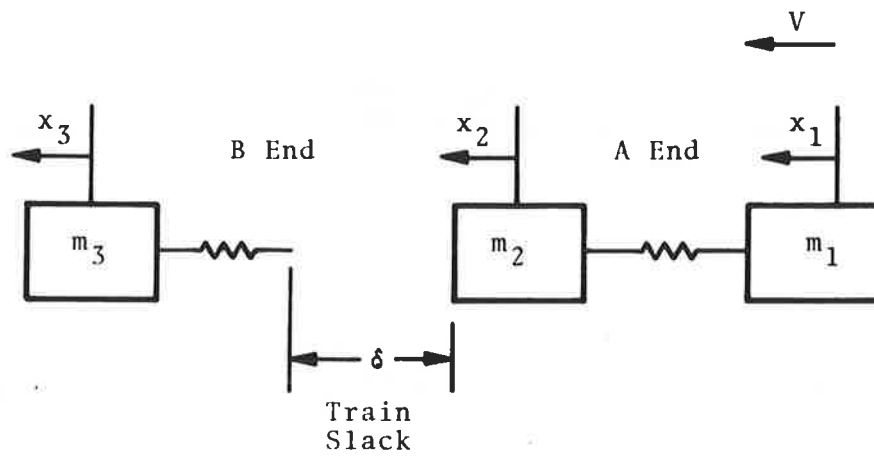


FIGURE 2. COLLISION OF THREE MASSES

longitudinal stiffnesses, and  $\delta$  is the gap\* between  $m_2$  and  $m_3$ . The car  $m_1$  impacts on  $m_2$  with a speed  $V$  at time  $t=0$ . Frequently the impacting car is a locomotive and the impacted car is a caboose.

Assuming an elastic impact, the approximate solutions (Appendix A) for the longitudinal forces are:

$$\begin{aligned} F_1(t) &= k_1(x_1 - x_2) = V \sqrt{k_1 m} \sin \omega_0 t \\ F_2(t) &= 0 \end{aligned} \quad (1)$$

for  $0 \leq t \leq t_0$ , where  $t_0$  represents the time at which the slack is taken up between the impacted car and the backup car.

For  $t \geq t_0$ , the solutions are somewhat more complicated and are given in Appendix A, (see Eq. (A.6)). There are two longitudinal force components. One has a low frequency  $\Omega$  which relates to the oscillation of the two heavy masses  $m_1$  and  $m_3$ , and the other has a high frequency  $\omega$  which relates to the rapid oscillation of the light mass  $m_2$  between the two heavy masses. The ratio of the magnitudes of the two components is of order  $\sqrt{m_2/m_1}$ .

It is clear that the forces are linearly proportional to the impact velocity,  $V$ , and the square root of the stiffnesses and the effective masses. The forces also depend on the time at which the impacted car strikes the backup car. This depends on the distance between  $m_2$  and  $m_3$  and initial impact velocity on  $m_2$ . The maximum impact force on the impacted car is approximately

$$F_{\max} \cong V \left[ \sqrt{\frac{k_1 k_2}{k_1 + k_2} \frac{m_1 m_3}{m_1 + m_3}} + \frac{1}{2} \sqrt{\frac{k_1^2 m_2}{k_1 + k_2}} \right] \quad (2)$$

\*The spring characteristics look more like that shown in Fig. 19. The first portion represents the draft gear which is strain rate sensitive. However, the spring rate is relatively small compared to that of the second portion. In this section, we shall approximate the first portion by zero and use the second portion only. Therefore the gap  $\delta$  between  $m_2$  and  $m_3$  is actually the possible slack plus the draft gear travel of the two cars.

In using (2) to estimate the maximum impact force, the required information on the masses is generally available, or one can simply weigh the cars involved. The information on the stiffnesses is usually lacking, but it can be estimated with reasonable accuracy by considering the major structural component (i.e., the center sill).

It can be seen from Eqs. 1 and 2 that the maximum force is proportional to the impact velocity, and the square root of the effective stiffness such as  $k_1 k_2 / (k_1 + k_2)$  and that of the effective mass such as  $m_1 m_2 / (m_1 + m_2)$  and  $m_1 m_3 / (m_1 + m_3)$ . This result can be generalized to the case of a collision of trains with many cars. It is the impact velocity, the stiffness and the mass of each individual car determining the magnitude of the force rather than the total mass of a train. For example the maximum impacting force on the impacted car of a train will be about the same whether it is impacted by a one-car train or by a hundred-car train of similar cars. However, the impulse on the impacted train does depend on the total mass.

Now consider an example with\*

$$\begin{aligned}
 m_1 &= 250000/g && \text{lb-sec}^2/\text{in} \\
 m_2 &= 30000/g && \text{lb-sec}^2/\text{in (without trucks)} \\
 m_3 &= 160000/g && \text{lb-sec}^2/\text{in} \\
 k_1 &= k_2 = 0.3 \times 10^6 && \text{lb/in} \\
 g &= 386.4 && \text{in/sec}^2 \\
 V &= 13 \text{ mph} = 229 && \text{in/sec} \\
 \delta &= 1.8 && \text{in}
 \end{aligned} \tag{3}$$

Following the procedure outlines in Appendix A, we have:

$$\begin{aligned}
 \omega_0 &= 66 \text{ rad/sec} \\
 \omega &= 93 \text{ rad/sec}
 \end{aligned}$$

---

\*These are the approximate parameters for a rear end collision where a locomotive impacts into a caboose.

$$\Omega = 24 \text{ rad/sec}$$

$$t_0 = 0.024 \text{ sec}$$

and

$$F_1(t) = 1.05 \times 10^6 \sin(66t)$$

$$F_2(t) = 0$$

for  $t \leq 0.024 \text{ sec}$  and

$$F_1(t) \cong 1.4 \times 10^6 \sin(\Omega t - .35) + 0.68 \times 10^6 \sin(\omega t - .96)$$

$$F_2(t) \cong 1.4 \times 10^6 \sin(\Omega t - 0.35) - 0.68 \times 10^6 \sin(\omega t - 0.96) \quad (4)$$

for  $t > 0.024 \text{ sec}$ . The amplitude of  $F_1(t)$  is  $1.05 \times 10^6 \text{ lbs}$  for  $t \leq t_0$ . This would be maximum force experienced by the impacted car if there is no backup car. However, at  $t=t_0$ ,  $m_2$  impacts on the freight car, the forces on  $m_2$  have two components with amplitudes of  $1.4 \times 10^6 \text{ lbs}$  and  $0.68 \times 10^6 \text{ lbs}$ , associated with frequencies of 24 rad/sec and 93 rad/sec respectively. The forces can reach a maximum value of  $1.8 \times 10^6 \text{ lbs}$  within the period of impact.

The longitudinal forces  $F_1$  and  $F_2$  are plotted in Figure 3. After  $m_1$  impacts on  $m_2$ , the first peak of the forces occurs at the A end (between  $m_1$  and  $m_2$ ), which is called the first impact. In the meantime,  $m_2$  is being pushed forward and impacts on  $m_3$ , and the second peak of the forces occurs at the B end between  $m_2$  and  $m_3$ , which is called the second impact. After impacting on  $m_3$ ,  $m_2$  slows down and bounces back, and while  $m_1$  is catching up, a third peak force occurs at the A end, which is called the third impact. Such a process continues as  $m_2$  oscillates between the two heavy cars. It is interesting to note that the force amplitude for each impact increases initially and then decreases. This solution is based on an elastic analysis. The actual maximum value will be limited by the yield-strength of the car when structural failure occurs.

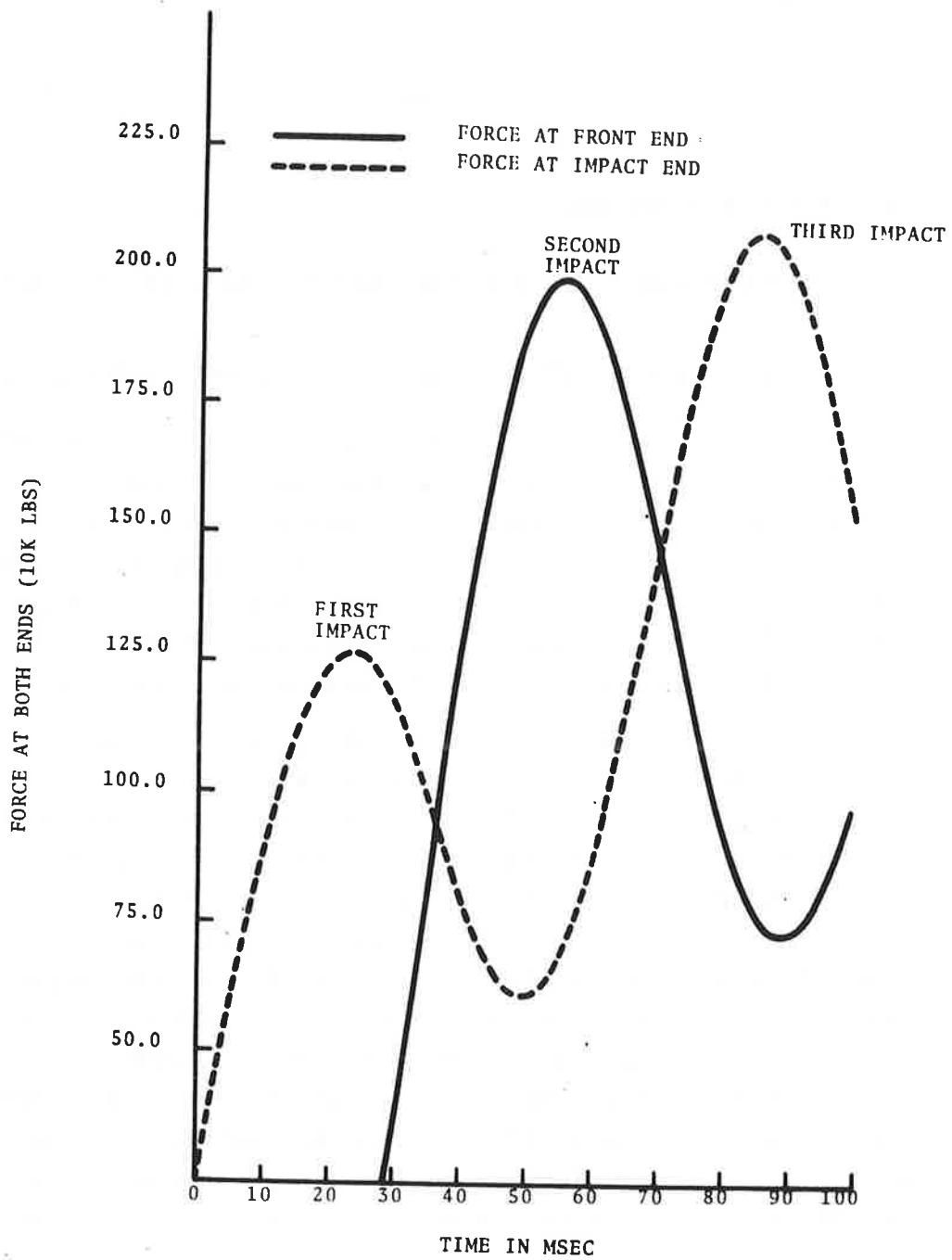


FIGURE 3. LONGITUDINAL FORCES AT BOTH ENDS

## 2.2 ESTIMATION OF THE VERTICAL AND PITCH MOTIONS OF THE IMPACTED CAR

The longitudinal forces derived previously act at the coupler faces, which are usually below the center of gravity of the impacted car (Figure 4) so that pitch and vertical motions are induced. We shall estimate such motions for the case of no backup car. The approximate solutions at time  $t_0$  are (see Appendix A for detailed derivation):

$$v_0 + \ell \theta_0 = \frac{A}{\omega_0} \frac{\sin \alpha \pi}{\alpha(\alpha^2 - 1)} = \frac{A}{\omega_0} f(\alpha)$$

$$v_0 = \frac{A}{\omega_0 \left(1 + \frac{\ell^2 m_2}{I_2}\right)} \left[ \frac{\sin \alpha \pi}{\alpha(\alpha^2 - 1)} \right] + \frac{eVm\pi}{m_2 \omega_0} \quad (5)$$

and the corresponding velocities are

$$\dot{v}_0 + \ell \dot{\theta}_0 = A \frac{(1 + \cos \alpha t)}{\alpha^2 - 1} = A g(\alpha) \quad (6)$$

$$\dot{v}_0 = \frac{A}{1 + \ell^2 \frac{m_2}{I_2}} \left[ \frac{1 + \cos \alpha t}{\alpha^2 - 1} + 2 \right] + \frac{2eVm}{m_2}$$

where (see also Figure 4):

$\alpha = \omega_v / \omega_0$  = Ratio of the natural frequency of the impacted car in pitch pivoted at the impacted end to the natural frequency for longitudinal oscillation between the two cars.

$e$  = Misalignment angle of the longitudinal force which may be caused by a difference in coupler heights.

$I_2$  = Rotary inertia of the impacted car.

$\ell$  = Half the distance between the two trucks.

$L$  = Half the car length.

$h$  = Vertical distance between the car c.g., and the coupler centerline.

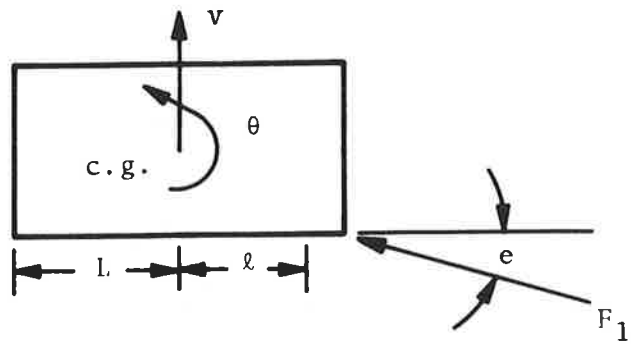


FIGURE 4. INDUCED VERTICAL AND PITCHING MOTION AFTER IMPACT

$$m = m_1 m_2 / (m_1 + m_2)$$

$$A = \frac{Vm}{I_2} \left[ \ell h - e \left( \frac{I_2}{m_2} + \ell L \right) \right]$$

Equations (5) and (6) clearly show that the sign of A determines the direction of the vertical and pitching motions, and this sign is determined in turn by coupler misalignment. Plots of the functions  $f(\alpha)$  and  $g(\alpha)$  in Eqs. (5) and (6) with  $e=0$  are given in Figure 5. It is clear that  $v_o$  and  $\theta_o$  tend to an asymptotic value of order  $1/\alpha^3$  while  $\dot{v}_o$  and  $\dot{\theta}_o$  tend to asymptotic value of order  $1/\alpha^2$  as  $\alpha \rightarrow \infty$ .

It is of interest to determine the maximum possible vertical displacement of both ends of the caboose. Equation (A.12) describes the motion for the time period  $0 \leq t \leq \pi/\omega_o$  before  $m_2$  separates from  $m_1$ . After separation, the motion of the impacted car involves only the interaction of the car body and its trucks. We shall consider an extreme case with  $\omega_v \gg \omega_o$  and  $\omega_t$  is large and  $e=0$  (Appendix A). This is the case where the vertical spring constants of the center sill and the truck are stiff and when there is no misalignment. From Eq. (5), at  $t = \pi/\omega_o$ , we have

$$v_o + \ell \theta_o = 0$$

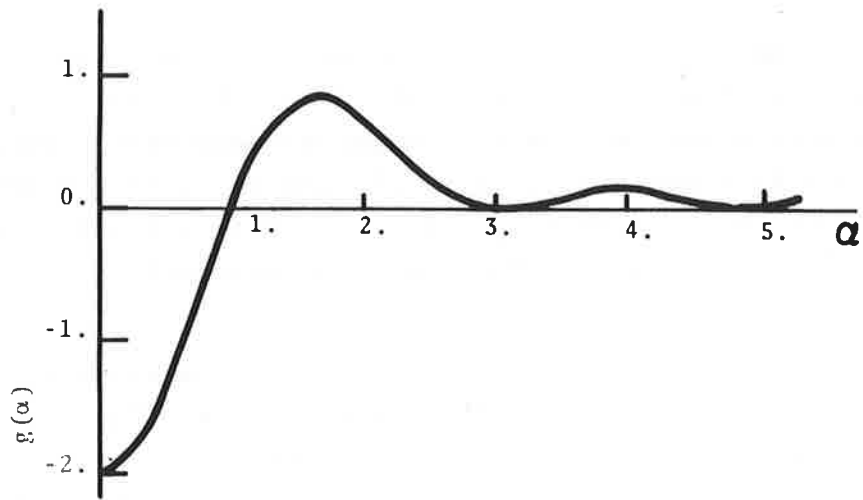
$$v_o = \frac{\pi \ell h Vm}{\omega_o (I_2 + \ell^2 m_2)} \quad (7)$$

Also from Eq. (6), we have

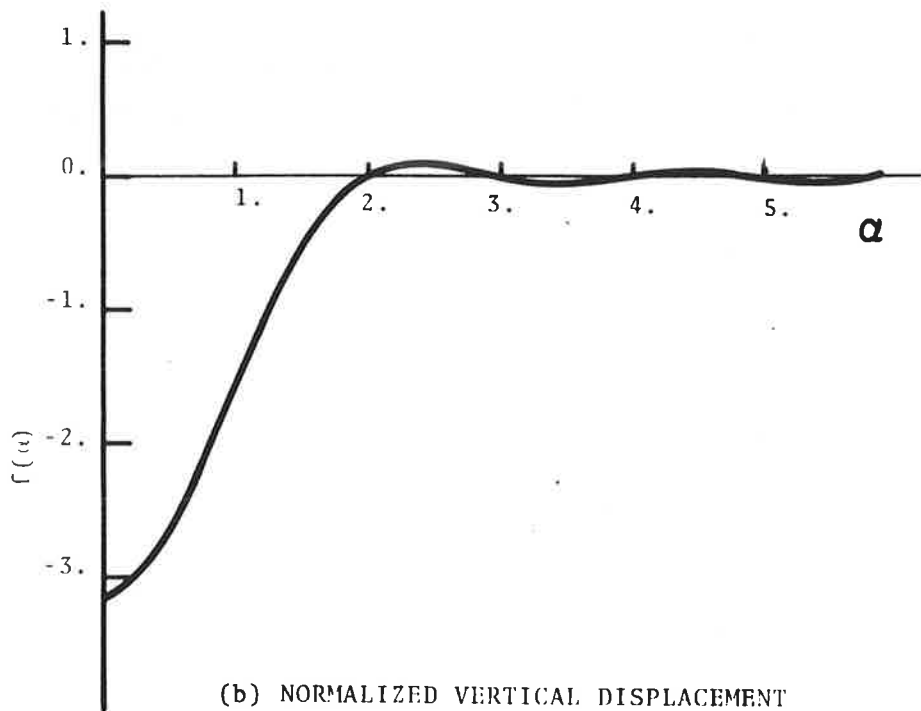
$$\dot{v}_o + \ell \dot{\theta}_o = 0$$

$$\dot{v}_o = \frac{2 \ell h Vm}{I_2 + \ell^2 m_2} \quad (8)$$

The maximum vertical displacement,  $v$ , can be easily evaluated from (A.16). At time



(a) NORMALIZED VERTICAL VELOCITY



(b) NORMALIZED VERTICAL DISPLACEMENT

FIGURE 5. NORMALIZED VERTICAL VELOCITY AND DISPLACEMENT

$$t = \frac{\pi}{\omega_0} + t_m = \frac{\pi}{\omega_0} + \frac{2hVm}{m_2 \ell g}, \quad (9)$$

we have

$$\begin{aligned} v_{\max} &= \frac{1}{2} \frac{\dot{v}_0^2 (I_2 + m_2 \ell^2)}{m_2 \ell^2 g} + v_0 \\ &= 2h^2 v^2 m^2 / \left[ m_2 g (I_2 + m_2 \ell^2) \right] + \frac{\pi \ell h V m}{\omega_0 (I_2 + m_2 \ell^2)} \end{aligned} \quad (10)$$

The corresponding displacements at the front end and the impact end are, respectively:

$$\begin{aligned} v_F &= \frac{\ell+L}{\ell} v_{\max} \\ v_I &= \frac{\ell-L}{\ell} v_{\max} \end{aligned} \quad (11)$$

The horizontal displacement and velocity of  $m_2$ , can be evaluated from Eq. (A.3), i.e., at  $t=\pi/\omega_0$ ,

$$\begin{aligned} u_0 &= \frac{V m_1}{m_1 + m_2} \frac{\pi}{\omega_0} \\ \dot{u}_0 &= \frac{2 m_1 V}{m_1 + m_2} \end{aligned}$$

For  $t > \pi/\omega_0$ , the horizontal velocity will be slowed down somewhat by its two trucks and is estimated to be\*

\*The estimate of  $u_1$  is somewhat on the high side. Since during impact, the trucks, in particular, the one near the impact end, have interaction with  $m_2$ . In general, one may use the estimate

$$\dot{u}_1 = \dot{u}_0 \frac{m_2 - 2am_t}{m_2 + 2m_t}$$

where  $a$  is some constant such that  $-1 < a < 1$ .

$$\dot{u}_1 = \dot{u}_0 \frac{m_2}{m_2 + 2m_t} \quad (12)$$

where  $m_t$  is the mass of one truck. The horizontal displacement when  $v$  reaches its maximum is

$$u_1 = u_0 + \dot{u}_1 t_m = \frac{Vm_1}{m_1 + m_2} \left[ \frac{\pi}{\omega_0} + \frac{4hVm}{lg(m_2 + 2m_t)} \right] \quad (13)$$

From (A.16), the vertical displacement of  $m_2$  falls to zero at approximately

$$t = \frac{\pi}{\omega_0} + 2t_m$$

and the corresponding horizontal displacement is

$$u_2 = u_0 + 2t_m \dot{u}_1 = \frac{Vm_1}{m_1 + m_2} \left[ \frac{\pi}{\omega_0} + \frac{8hVm}{lg(m_2 + 2m_t)} \right] \quad (14)$$

From the above analysis, one should note that  $v_{\max}$ ,  $u_1$ , and  $u_2$  are all proportional to the square of the impact velocity.

Using the numerical values for  $m_2$ ,  $k_1$ , etc. in Eq. (3) and

$$L = 200 \text{ in.}$$

$$l = 150 \text{ in.}$$

$$h = 20 \text{ in.}$$

$$I_2/m_2 = 10000 \text{ in}^2$$

we obtain, from (7) and (8)

$$v_0 = 0.9 \text{ in.}$$

$$\dot{v}_0 = 38 \text{ in./sec.}$$

with the value

$$v_{\max} = 3.5 \text{ in.}$$

A substitution of  $t$  and  $v_{\max}$  into (12) yields

$$\begin{aligned} v_F &= 8 \text{ in.} \\ v_I &= - 1.2 \text{ in.} \end{aligned} \tag{15}$$

For a truck of weight 7000 lbs (i.e.,  $m_t = 18 \text{ lbs-sec}^2/\text{in.}$ ), we have

$$\begin{aligned} u_1 &= 51 \text{ inches} \\ u_2 &= 91 \text{ inches} \end{aligned} \tag{16}$$

A plot of  $u_1$  and  $u_2$  vs the impact velocity is given in Figure 6.

### 2.3 EFFECT OF MISALIGNMENT

From Eq. (A.9) or (A.11) if the misalignment is sufficiently large, i.e.

$$e > \frac{h}{L} \tag{17}$$

the moment about the center of gravity due to the longitudinal force changes sign. The impact end of the car body will pitch up rather than down. In other words, the subsequent motion of the car body after separation will be pivoted about the front truck.

Consider a simple case where  $e=h/L$  and  $k_t, k_v \ll k_1$  (this is equivalent to  $\omega_t \ll \omega_0$ ). The approximate solution Eqs. (5) and (6) at  $t=\pi/\omega_0$  is

$$\begin{aligned} v_0 &= \frac{eVm\pi}{m_2\omega_0} \\ \dot{v}_0 &= \frac{2eVm}{m_2} \\ \theta_0 &= \dot{\theta}_0 = 0 \end{aligned} \tag{18}$$

That is the impacted car moves up vertically without pitching after separation from the impacting car. The maximum height of the impacted car will be

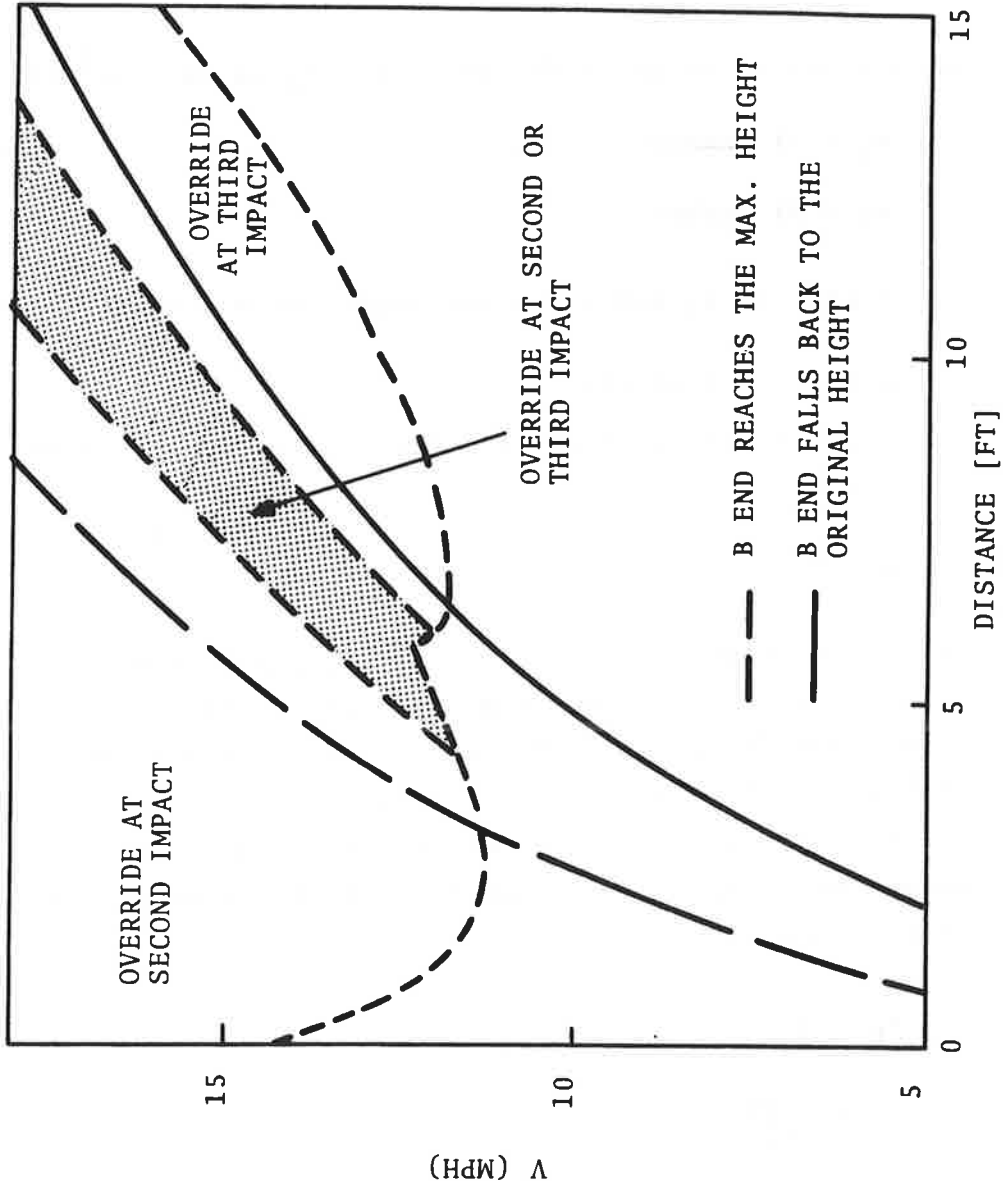


FIGURE 6. OVERRIDE MODES VS. IMPACT SPEED FOR THE PARAMETERS GIVEN IN EQUATION 3

$$v_{\max} = \frac{1}{2} \frac{v_o^2}{g} + v_o$$

Using the parameters Eq. (3), we have

$$e = 0.1$$

$$v_{\max} = 3 \text{ in.}$$

If the distance of the draft gears between two impacting cars is 50 inches, and  $e=0.1$ , the coupler on  $m_2$  will be about 5 in. higher than that of the impacting car  $m_1$ . When  $m_2$  moves up an additional 3 inches, its coupler almost clears the coupler of  $m_1$ .

### 3. MECHANISM OF OVERRIDE

Override in a train collision is a phenomenon where the stiff part of a car body such as the center sill or the floor impacts on the superstructure of another car. The superstructure is in general much weaker than the sill. Override will result in penetration into the overridden car, or extensive crush of the superstructure of the overridden car, while little or no damage to the overriding car occurs. Evidently override is due to the difference in vertical motions in the cars during impact which results in a mismatch of the stiff parts of the two cars. The mechanism of the override can be understood if we understand the causes of the vertical motion and why cars have different vertical motions in impact.

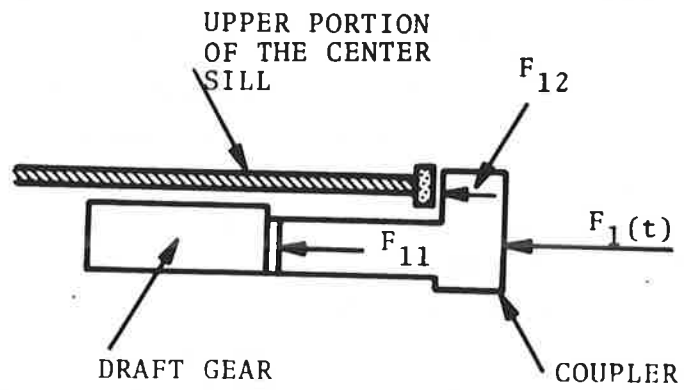
From the analysis of the last section, it is clear that a large longitudinal force is developed during impact of two rail cars. This force is applied at the coupler faces, which are generally below the center of gravity of the car (except for the case where the impacted car is an unloaded flat car). A moment of  $hF_1(t)$ , (see Eq. A-9) about the c.g. will result causing the other end to pitch up. Due to the vertical constraint of the car itself, the pitching motion may induce a subsequent vertical motion.

There is another mechanism which causes a car to move vertically and to pitch. The longitudinal forces are, in general, not parallel to the ground (mainly due to misalignment of the impacting couplers). A small deviation from the horizontal direction will result in a large vertical force. For example, if a longitudinal force  $F(t)$  of magnitude of  $10^6$  lbs has a 5.7 degree angle off the horizontal line (i.e.,  $e=0.1$ ), it will have a vertical component,  $eF(t)$ , of 100,000 lbs. This force can produce a 3.3g acceleration in the vertical direction for a car weighing 30,000 lbs. Besides, this force acts at the end of the car, and has a large moment arm,  $L$ , which is roughly half of the car length, to the car center of gravity. This resulting moment is  $eLF(t)$  which can cause a large

pitching acceleration. For the case  $e=0.1$ ,  $L=200$  in., and a rotary inertia of  $760,000$  lb-in/sec<sup>2</sup>, the pitching acceleration can be as high as  $26$  rad/sec<sup>2</sup>.

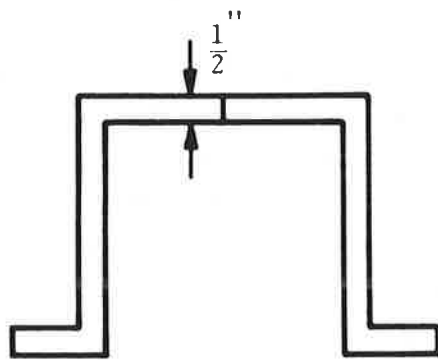
The orientation of the longitudinal forces is affected initially by the alignment of the coupler height at the time prior to impact (see A.9, and A.10), and it will also be affected by the deformation and the motion during impact. At a sufficiently high speed impact or in the case of a car with a worn out draft gear, the coupler horn can hit the striking plate. In this situation, a part of the longitudinal force will pass through the striking plate to the center sill (Figure 7). This has the effect of increasing the height of the point where the longitudinal force is applied and thus reduces the effective c.g. height; the force on the coupler horn creates a local moment rotating the coupler, which will change the direction of the longitudinal force and is equivalent to the changing of the effective misalignment.

There is still another situation that can change the effective misalignment drastically and enhance the vertical motion during impact, and that is the buckling or the plastic deformation of a major structural component such as the center sill, the draft gear, or the coupler shank. These are usually the major structural members transmitting the longitudinal load. The cross-sectional shapes of the sill and the shank are shown in Figure 8. They both have an area approximately of 20 to 23 inch-square. The structural steel for these parts has a yield stress of about 40,000 to 60,000 psi. Therefore the yield strength is about  $0.9 \times 10^6$  to  $1.4 \times 10^6$  lbs. This means that for the 13 mph impact discussed in Section 2, the longitudinal force can exceed the yield strength and can result in plastic deformation. Once yielding occurs, the bending characteristics change drastically. In fact, these structures are made of a mild steel which has little strain hardening during plastic deformation. Upon yielding under axial load, the bending rigidity reduces essentially vanishes. The sill or the coupler shank can easily buckle resulting in a large rotation which will have two effects. First, the lowering of the bending rigidity constitutes a reduction of the stiffness in the vertical direction,

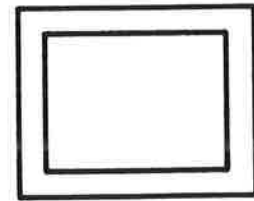


$$F_1 = F_{11} + F_{12}$$

FIGURE 7. TRANSMISSION OF LONGITUDINAL FORCES



a. Center Sill



b. Coupler Shank

FIGURE 8. CROSS-SECTION OF THE CENTER SILL AND THE COUPLER SHANK

which means reducing the restraints for the vertical movement. This is clear from examining Eq. (A.9) where  $k_v$  is actually an approximation of the bending of the sills, the coupler shanks and the components in the draft gears. Secondly, the large rotation is effectively a change in the misalignment which reorients the longitudinal force and results in large vertical component of the force inducing further vertical movement.

We can see that the major causes for the induced vertical and pitch motions are the misalignments of the longitudinal forces from the center of gravity and from the horizontal direction. The direction and the amplitude of the vertical and the pitch motion depend on the mass, the rotary inertia, the c.g. location, the size of the misalignment, the stiffness in the vertical direction, the impact speed, the number of cars involved, and the strength of the various components such as the center sill, the draft gear and the coupler shank. The masses, the moments of inertia and the c.g. locations of two impacting cars are generally different. The longitudinal forces on the other ends of these two cars can also be different. Therefore the amplitude and the direction of their induced vertical and pitching motions are usually not the same, which can result in slippage between the two impacting coupler faces. When the slippage is large enough such that the coupler of one car clears the height of the coupler of another car, override will occur.

We can now summarize the factors which contribute to the override of car 1 on car 2. These, shown schematically in Figure 9, are:

1. The longitudinal force at the B end of car 1 causes the A end to pitch up.
2. At the A end, car 1 has an upward velocity with respect to car 2.
3. At the A end, the coupler of car 1 is higher than that of car 2 and/or the coupler horn of car 1 hits striker plate which causes the vertical component of the longitudinal force between the cars pointing upward on car 1.

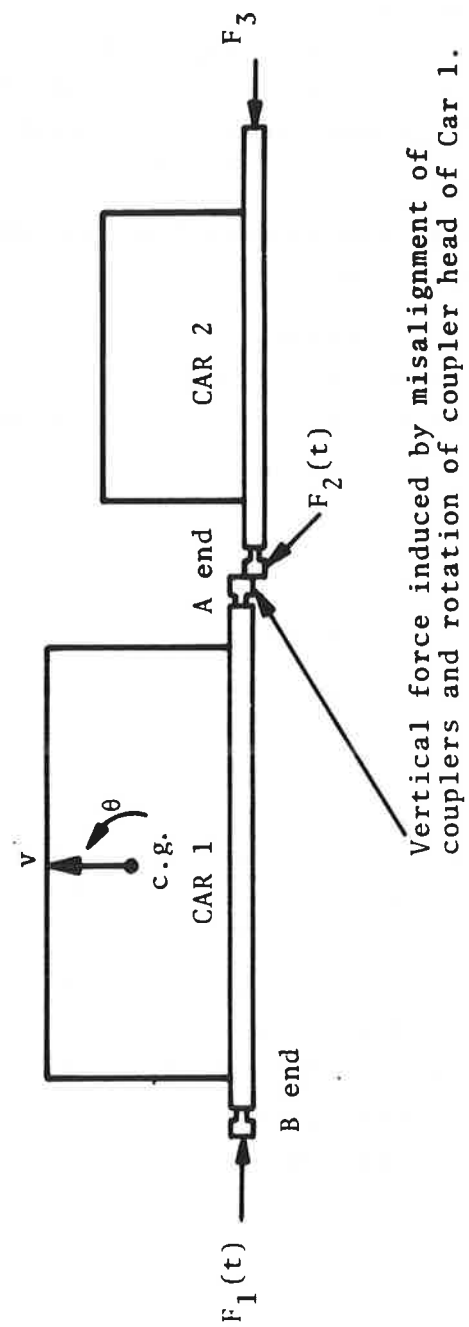


FIGURE 9. FACTORS CONTRIBUTE TO OVERRIDE ON CAR 2

4. At the A end, the coupler shank and/or the sill of car 1 or car 2 yields and rotates which results in the impacting force pointing upward on car 1.

The evaluation of the contribution of each of these factors to an override in a multiple-car collision is quite complicated. One often must resort to numerical means. A more detailed discussion of the numerical computations will be presented in the next section.

We shall now discuss the circumstances leading to different kinds of override.

Case 1 - Override of  $m_2$  on  $m_1$  at the first impact (Fig. 1.2).\* This is an override occurs after  $m_1$  impacts on  $m_2$  before or just barely after  $m_2$  impacts on  $m_3$ . Normally when  $m_1$  impacts on  $m_2$ , the longitudinal force between the two cars will cause them to pitch down at the A end. However there are circumstances which will cause the impact end to move up clearing the coupler of  $m_1$  if the impact speed is sufficiently high. These circumstances are: (a) The initial misalignment is large enough to satisfy  $e > h/L$ . (b) During impact, the effective misalignment due to deformation (such as the coupler horn of  $m_2$  hitting the striker plate or the combined bending and compression of the longitudinal force causing yielding and rotation of the coupler shank or the center sill) is large enough so that  $e > h/L$ . In case (a), the magnitude of misalignment depends on what type of car  $m_2$  is. For example, if  $m_2$  is a caboose,  $h/L$  is approximately equal to 0.1, which requires that the coupler of  $m_2$  be about 5 inches higher than that of  $m_1$ . However, if  $m_2$  is a light flat car,  $h$  is approximately zero. Then very little misalignment is needed for  $e > h/L$ . Case (b) is more likely to happen if  $m_2$  is a heavy car. This is because a larger longitudinal force will develop causing yielding

---

\*The situation when  $m_1$  overrides on  $m_2$  at the first impact is similar. This can be visualized if one imagines an observer moving at a speed  $V$  with  $m_1$ . In this case the roles played by  $m_1$  and  $m_2$  as discussed in this section are reversed.

as compared to the case of a light  $m_2$ . In both cases, little misalignment is required if  $h$  is small.

Case 2 - Override of  $m_2$  and  $m_3$  at the second impact (Fig. 1.3). This is an impact of  $m_2$  at the A end causing its B end to override on  $m_3$ . If the coupler height of  $m_2$  is not much higher (i.e.,  $e < h/L$  in Eq. A.9) or is lower than that of the impacting car  $m_1$ ,  $m_2$  will pitch up at the B end. The pivot point is more or less at the impact end truck. An override on  $m_3$  will occur if either one of the following events happens within the period of second impact when  $m_2$  is crushing on  $m_3$ : (a) The B end of  $m_2$  is very high so that when  $m_2$  reaches  $m_3$  its coupler already clears the coupler of the  $m_3$ . (b) The B end of  $m_2$  is high enough such that the misalignment between  $m_2$  and  $m_3$  can cause the longitudinal force between these two cars to push  $m_2$  upward further until its coupler clears that of  $m_3$ . (c) The B end of  $m_2$  has enough vertical velocity to continue moving upward to clear the coupler of  $m_3$ .

In case (a), it is likely that there is a large initial misalignment between  $m_2$  and  $m_3$  and/or that there is sufficient distance between  $m_2$  and  $m_3$ . In the latter situation, there will be time for the B end of  $m_2$  to move up high enough when  $m_2$  impacts on  $m_3$ . This distance traveled by  $m_2$  when it reaches the maximum height is estimated in Eq. 13. The distance is plotted in Figure 6 for a given set of  $m_1$  and  $m_2$ . In order for  $m_2$  to move high up easily,  $m_2$  is likely to be a light car with a small rotatory of inertia.

Case (b) can happen for the same reasons as that of case (a). For example, in Section 2.2 for an impact of 13 mph on  $m_2$  by  $m_1$ , the B end of  $m_2$  can reach the maximum height of 8 in. During this time,  $m_2$  has traveled forward about 51 inches. If  $m_3$  is located at this distance ahead of  $m_2$ , with an 8 inch difference\* in coupler height, the impact of  $m_2$  on  $m_3$  can easily result in

---

\*The difference can be larger if there is an initial misalignment.

override on  $m_3$ . This case is more likely to happen, if  $m_2$  is a light car, and  $m_3$  is located at where the B end of  $m_2$  reaches its maximum height.

Case (c) is often the result of a sufficiently high speed impact at the A end of  $m_2$  which induces the vertical motion at the B end. This is the case where the distance between  $m_2$  and  $m_3$  is quite small. During the impact between  $m_2$  and  $m_3$ , the A end of  $m_2$  is still being pushed by  $m_1$  which provides a continuous input of energy to cause the override of  $m_2$  on  $m_3$ .

The occurrence of any one of the following two events during the impact between  $m_2$  and  $m_3$  will further enhance the chance of override. One is that the coupler horn at the B end of  $m_2$  hits the striker which is in effect an increase of misalignment. The other is that the combination of the longitudinal force between  $m_2$  and  $m_3$  and the bending moment is large enough to cause yielding of the coupling shank or the center sill causing a large rotation of the coupler (this will further enhance the misalignment to push  $m_2$  upward). In this situation, it is not necessary for  $m_2$  to be light as long as it carries sufficient momentum when impacting on  $m_3$ .

Case 3 - Override of  $m_2$  on  $m_1$  at the third impact (Fig. 1.2 or 1.4). Even though  $m_2$  pitches down initially at the A end after impact, if the pitch frequency is low enough and/or if the distance between  $m_2$  and  $m_3$  is large enough (say about the value of  $u_2$  defined in Eq. 14), the A end of  $m_2$  can be pitching up about the time of the third impact. If the A end experiences any one of the situations described previously in (2) for the B end of  $m_2$  in its relation to  $m_3$ , override on  $m_1$  can occur. That is, the case where the impact of the B end of  $m_2$  by  $m_3$  causes the A end to override  $m_1$ , is the same as  $m_1$  impacting the A end of  $m_2$  causing the B end to override  $m_3$  as discussed in (2). This is clear if one looks from the point of view of an observer moving with the same velocity as  $m_2$  after it separates from  $m_1$ . He sees  $m_2$  being impacted by  $m_3$  causing the opposite end to pitch up and resulting in an override. In other words, the first impact is merely

causing  $m_2$  to move, and the velocity of  $m_2$  in the impact direction is higher than  $m_1$ . As  $m_2$  moves toward  $m_3$ , the gap between  $m_2$  and  $m_1$  increases. When  $m_2$  impacts  $m_3$ , the impact will cause the A end of  $m_2$  to pitch up. The gap between  $m_2$  and  $m_1$  is sufficient in terms of time to allow the A end to move high enough before  $m_1$  can catch up to  $m_2$ , resulting in an override on  $m_1$ .\*

There is another situation where an override at the third impact can occur. When the B end of  $m_2$  pitches up after being impacted by  $m_1$ , the car body can lift up above the truck bowl, move forward and leave the B end truck behind. If the distance between  $m_2$  and  $m_3$  is sufficiently large (say  $>u_2$  of Eq. 14 for a given impact speed  $V$ ) and if the B end center plate does not return to the truck bowl when it falls down,\*\* the B end coupler of  $m_2$  can fall to a height which is below the coupler of  $m_3$  when  $m_2$  reaches  $m_3$ . In this case,  $m_2$  can underide  $m_3$  resulting in the A end pointing upward. When  $m_1$  catches up, it will be overridden. However the distance between  $m_2$  and  $m_3$  should not be too large. If the B end falls to the ground before  $m_2$  hits  $m_3$ , due to track irregularity,  $m_2$  may be bounced off the track before  $m_1$  can catch it up, and there will be no override.

---

\* If the distance is too small, say about the value of  $u_1$ , in Eq. 13, override may occur at the second impact. If the distance is much larger than  $u_2$ , two things may happen: (1) After the B end of  $m_2$  falls back on the truck, it can bounce up again. When  $m_2$  reaches  $m_3$ , the B end can be high enough to cause an override on  $m_3$ . (2) The B end may not fall back exactly to the truck bowl and the irregular shape of the bolster can cause a lateral movement. When  $m_2$  reaches  $m_3$ , the lateral misalignment can cause  $m_2$  to jackknife or derail.

\*\* This can probably happen only at a relatively high impact speed where the B end lifts up before its truck barely starts to move. Usually, after the B end moves up, its truck also moves forward at a lower speed than the car body. If the difference between the horizontal displacement of the truck and the car body is less than half of the distance between its two trucks when the B end falls back, it cannot create much tilt for the A end to point upward. The center sill being only 2 inches higher than the center plate, will sit on the truck bolster and prevent the car body from falling to the ground.

The override at the third impact requires that  $m_2$  pitches up first at the B end then at the A end. This will more likely happen if  $m_2$  is a light car and is separated at a sufficient distance from the rest of the train when impact occurs.

Figure 6 shows a plot of impact speed vs the distances  $u_1$  and  $u_2$  traveled by  $m_2$  when it reaches the maximum height and when it falls back to the original position. It also gives the approximate regions where override is likely to occur at the second and at the third impact for the parameters given in Section 2 with no initial misalignment. This is a case of a heavy car  $m_1$  impacting on a light car  $m_2$  backed by a heavy car  $m_3$ . The values used for the yield strength of the coupler and the center sill are  $1.4 \times 10^6$  lbs in compression and  $3 \times 10^6$  in.-lbs in bending. The impact speed of  $m_2$  and  $m_3$  is given in Eq. (12) with an induced misalignment computed from (A.16). The override is predicted by using the finite element model described in Appendix B. For the region to the right of the curve  $u_2$  of Fig. 6, it is assumed that the B end truck moves along with  $m_2$  and the B end does not fall to the ground and there is no or little lateral motion to cause jackknifing. This plot covers only the range of moderate impact speed (say  $< 20$  mph). For the case of high speed collision, the increased structural deformations occur during impact which will have significant effects on the mechanism of override. It is interesting to note that there are two relative minima below which override is unlikely to occur for the given set of parameters when there is no misalignment. The minimum impact speed for override is likely at the second impact.

Case 4 - Buckling and crushing of the impacted car  $m_2$  (Figs. 1.5 and 1.6). If there is little misalignment (say the differences in coupler height between  $m_1$  and  $m_2$  and between  $m_2$  and  $m_3$  are less than 3 inches),  $m_2$  is closely backed up by the front car  $m_3$  and if the vertical stiffness between  $m_1$  and  $m_2$  and that between  $m_2$  and  $m_3$  are high, the pitching motion of  $m_2$  will be greatly restrained. A relatively high speed collision will result in buckling or crushing of the impacted car  $m_2$  as shown in Figs. 1.5 and 1.6. There are many cars having a slot on the center sill for the brake

line. The slot is a weak point of the sill and often is the point at which buckling initiates. If  $m_2$  is a heavy car, buckling of the sill often takes place near the body bolster and results in a damage as shown in Figure 1-6.

Different types of override and the likely train configuration are summarized in Table 1. In a collision, one of a combination of override modes may occur.

TABLE 1. SUMMARY OF OVERRIDE MODES AND TRAIN CONFIGURATIONS

Override Mode	Causes	Likely initial Configurations
First impact (Fig. 1.2)	<p>Initial misalignment between two impacting cars.</p> <p>Yielding of the coupler and the center sill between two impacting cars during the first impact.</p>	<p>Light or heavy impacted car.</p> <p>Impacted car with low center of gravity</p>
Second impact (Fig. 1.3)	<p>Misalignment due to the vertical and pitching motions of the impacted car induced by the first impact.</p> <p>Yielding of the coupler on the center sill between the impacted and the back up car during the second impact.</p>	<p>Light impacted car.</p> <p>Moderate spacing (see Eq. 13) between the impacted and the back up car.</p>
Third impact (Fig. 1.4)	<p>Misalignment due to the vertical and pitching motions of the impacted car induced by the second impact.</p> <p>Yielding of the coupler on the center sill between the impacted and the impacting car during the third impact.</p>	<p>Light impacted car.</p> <p>Large spacing (see Eq. 14) between the impacted and the back up car.</p>
Buckling (Fig. 1.5)	<p>Buckling or plastic deformation of the center sill or the entire car body of the impacted car at high speed impact.</p>	<p>Light or heavy impacted car.</p> <p>Little or no gap between the impacted and the back up car.</p>

#### 4. NUMERICAL SIMULATION OF REAR END COLLISION OF TRAINS

A more accurate car model of cars is necessary to simulate the detail motion of trains in collision. References 3 and 4 model a railroad car (including the trucks) as a single rigid body and use a massless spring to simulate the draft gear action and the deformation of the trucks. The present analysis uses the modular approach of the finite element method.<sup>5</sup> This approach enables the modeling of different cars in the consist and different parts of a car with varying degrees of details. The model of a car is shown schematically in Figure 10, and a version of the model of a car body is shown in Figure 11. More detail description of the modeling and the associated numerical problems are given in Appendix B.

Many computer simulations of collisions of two trains have been carried out, only the results of two cases are presented in this report. The parameters used are given in Table 2. The data are to simulate the two full scale train to train impact tests of 18.1 mph and 30.3 mph.

These tests were conducted by the Dynamic Science under the direction of Transportation Systems Center sponsored by FRA. The train consists of the two tests are shown in Figures 12 and 13 respectively. The stationary cut of cars has a caboose as an end car. The moving cut of cars, headed by a locomotive, was pushed to the desired test velocity by another locomotive and then released at few hundred feet prior to the impact. Hand brakes were applied on the standing train with all cars in buff position (except for the 30.3 mph test for which the caboose was in draft position). Emergent brakes were set on the moving train at the instant of impact.

In the 18.1 mph test, no gross deformation in any of the car body where expected, therefore only rigid elements are used in the modeling of all the car bodies. The longitudinal forces on both ends of the caboose are shown in Figure 14. The solid lines are

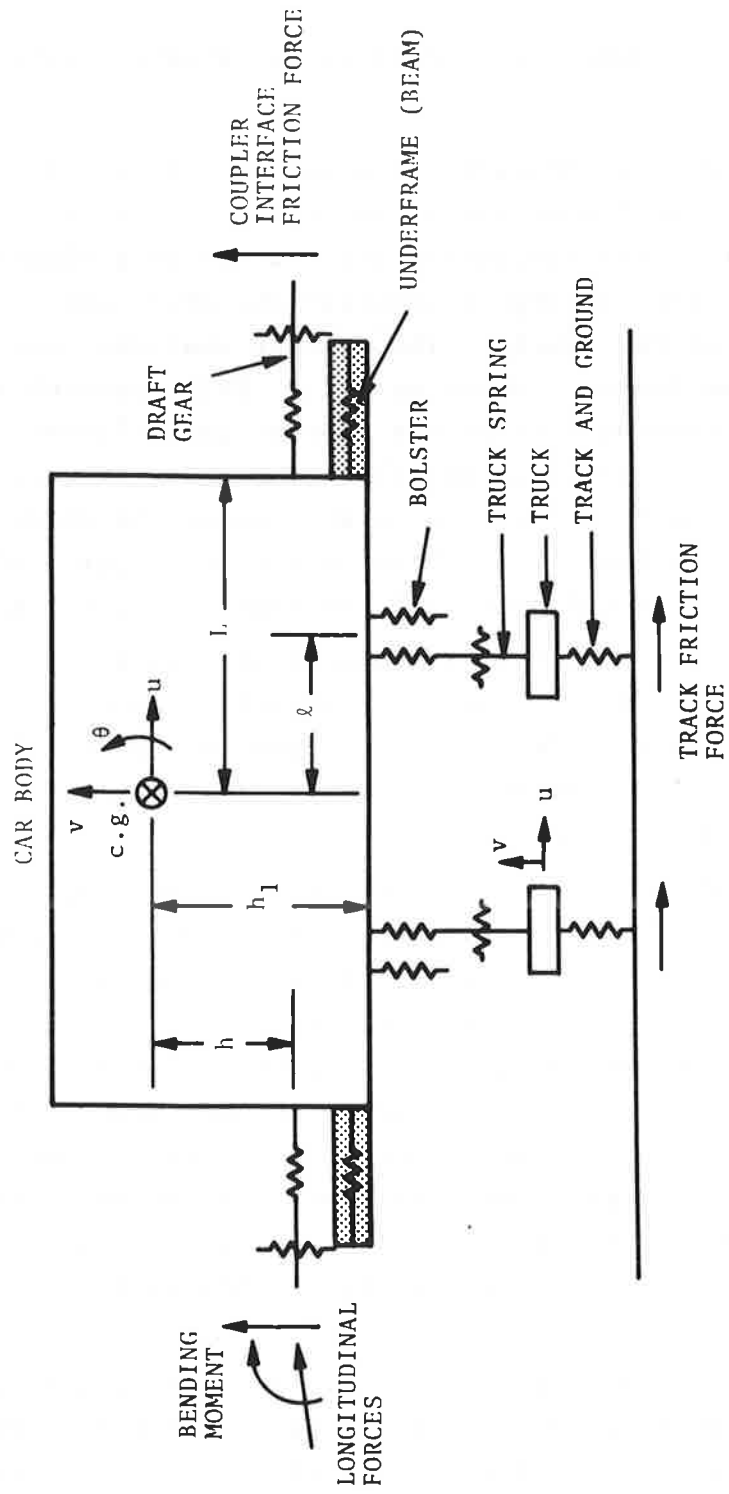


FIGURE 10. MATHEMATICAL MODEL OF A RAIL CAR

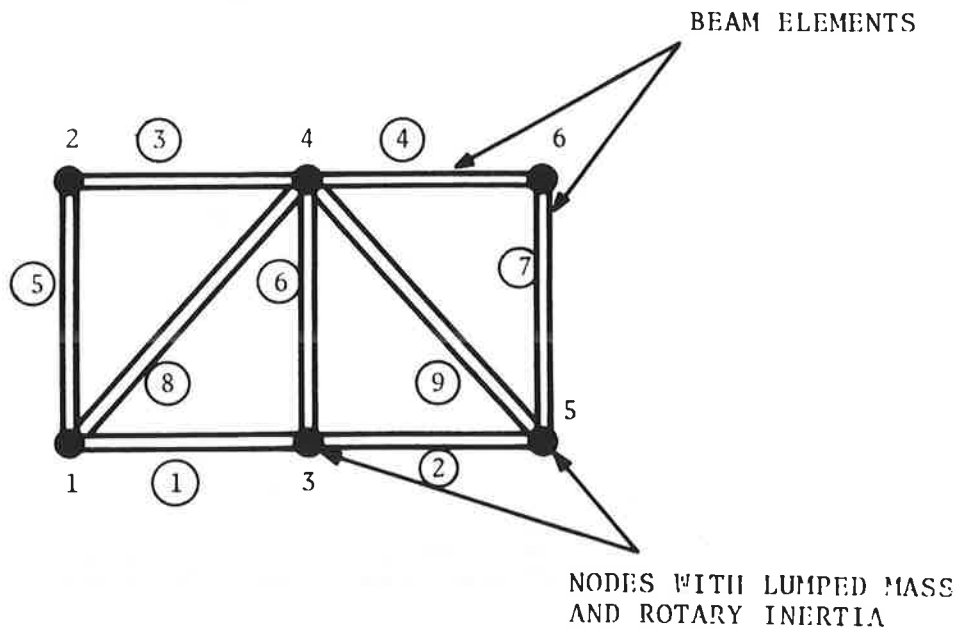


FIGURE 11. DETAIL MODELING OF A CAR BODY FOR HIGH SPEED IMPACT

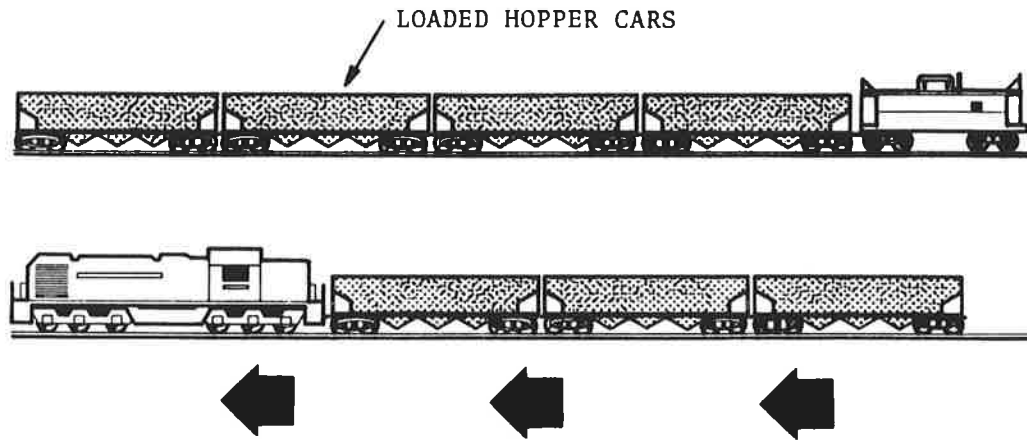


FIGURE 12. CUTS OF CARS FOR 18MPH REAR END COLLISION TEST

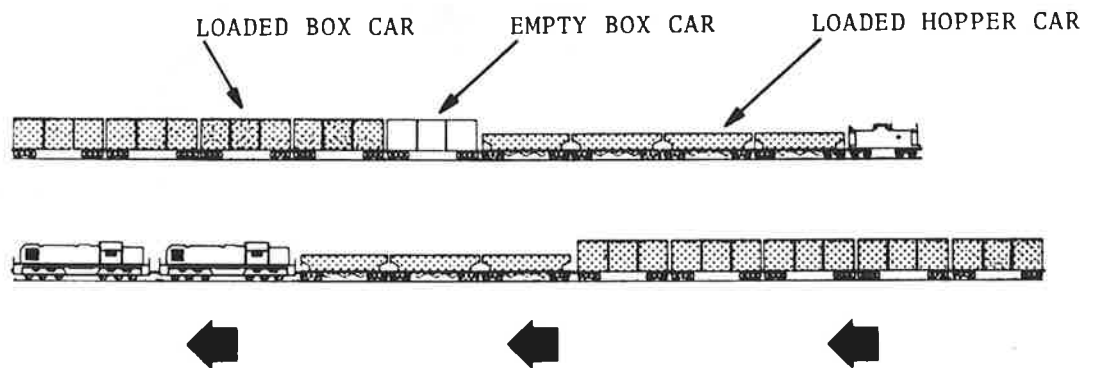
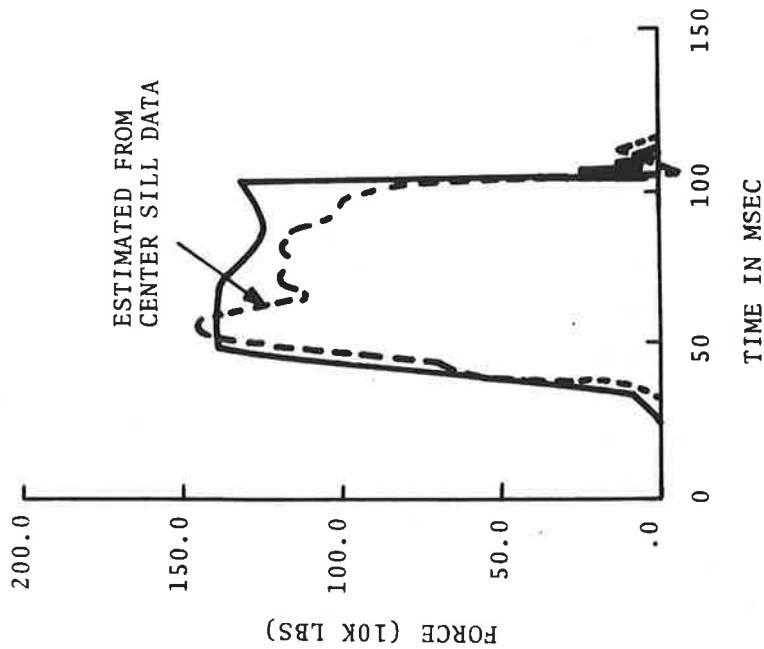
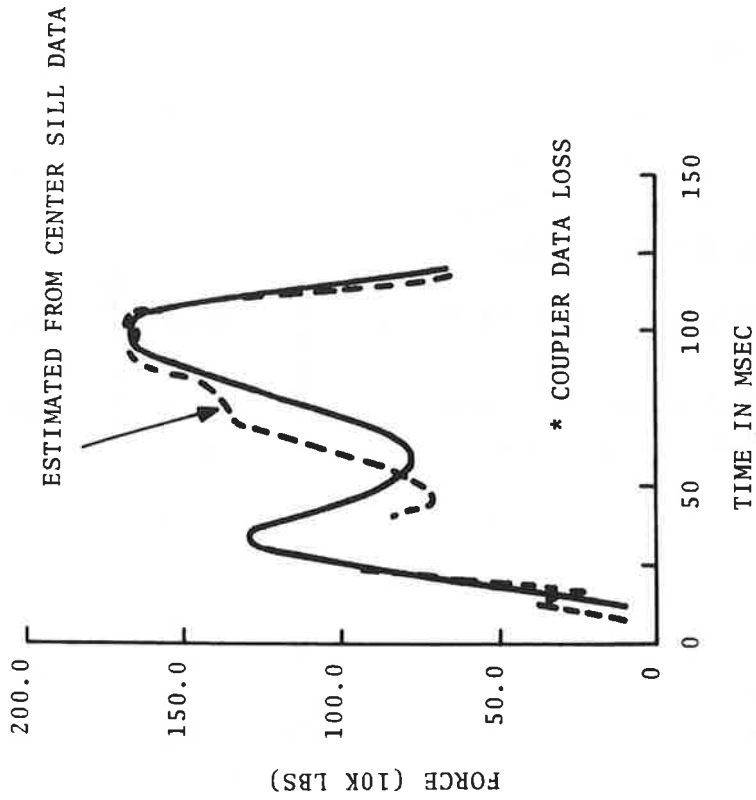


FIGURE 13. CUTS OF CARS FOR 30MPH REAR END COLLISION TEST



(a) FRONT END



(b) IMPACT END

FIGURE 14. LONGITUDINAL FORCES AT BOTH ENDS OF THE CABOOSE FOR 18.1 MPH IMPACT — COMPUTER SIMULATION --- FULL SCALE TEST

TABLE 2. PARAMETERS USED FOR TRAIN-TO-TRAIN IMPACT SIMULATION

CAR	CABOOSE	LOCOMOTIVE	CAR
CAR WEIGHT & LADING WT. (KIPS)	28.022	162.018	142.736
TRUCK SPRING WEIGHT (KIPS)	7.06	40.03	7.941
DISTANCE BETWEEN COUPLERS (IN)	304.	612.	446.
DISTANCE BETWEEN TRUCK SPRINGS (IN)	248.8	376.	300.
HT. FROM C.G. TO CENTER PLATE (IN)	32.43	40.25	41.88
HT. FROM C.G. TO COUPLERS (IN)	25.2	47.37	37.13
MASS MOMENT INERTIA (KIP-IN-SEC**2)	700.	19,230.	6450.
TRUCK VERT. SP. CONSTANT (KIP/IN)	8.084	50.	46.93
TRUCK HORIZ. SP. CONSTANT (KIP/IN)	250.	500.	250.
BOLSTER SP. CONSTANT (KIP/IN)	200	1500.	812.9
UNDERFRAME SP. CONST. (KIP/IN)	420(1260)*	1050.	1200.
UNDERFRAME YIELD LOAD (BENDING) (KIPS-IN)	3000.	3000.	3000.
UNDERFRAME YIELD LOAD (STRETCH) (KIPS)	1400.	1800.	1400.
DRAFT GEAR HORIZ. SP. CONST. (KIP/IN)	59.	60.	59.
DRAFT GEAR YIELD LOAD (STRETCH) (KIPS)	96.	96.	96.
VERT. COUPLER SPRING CONST. (KIP/IN)	50.	50.	50.
GROUND & TRACK SP. CONST (KIP/IN)	400.	600.	400.
DRAFT GEAR SPRING TRAVEL (IN)	1.75	4.0	3.
TRUCK SPRING TRAVEL (IN)	3.125	3.125	3.125
COUPLER VERTICAL SLACK (IN)	0.8	0.8	0.8
COUPLER HORIZONTAL SLACK (IN)	0.75	3.0	3.0
STRIKING VELOCITY	= 18.1	MPH	
COUPLER FACE (VERT.) FRICTION COEFFICIENT	= 0.08		
TRACK WHEEL FRICTION COEFFICIENT	= 0.2		
GROUND FRICTION COEFFICIENT	= 0.085		

\*Quantity in the parenthesis is used for 30.3 mph impact simulation.

numerical results and the dotted lines are those of the full scale test.\* The numerical simulation is terminated at 0.12 seconds. At this instant the caboose's coupler slipped off the coupler of the hopper car at the front end which is indicated in Figure 14a by the sudden drop of the longitudinal force at the front end (the B end). The slippage of the two couplers between the hopper car and the caboose is shown in Figure 15.

In the 30.3 mph test, the caboose was severely crushed and its center sill bent into a U-shape. In the simulation, we use the frame shown in Figure 11 to model the caboose body and rigid elements to model the rest of the car bodies. The additional parameters used in modeling the caboose by frame elements are given in Tables 3 and 4. The elements for the caboose are numbered as shown by the encircled numbers in Figure 11. The longitudinal forces on the caboose are plotted in Figure 16.

---

\*In the test, there are strain gages on the coupler shank and on the center sill (between the striker plate and the draft gear) to measure forces. Before the coupler horn hit the striker plate, all the longitudinal load, which is to be recorded by the gages on the coupler shank, is transmitted through the coupler shank to the draft gear and then to the center sill. After the horn hits the striker, a part of the load passes from the horn directly to the center sill which is to be recorded by the gages on the sill. During the test, the strain gages on the coupler shank at the impact end overcharged at about 0.025 seconds after the impact and those at the hopper car end of the caboose did not work at all. The force magnitude at the impacted end after 0.025 seconds and at the hopper car end are estimated from the center sill data.

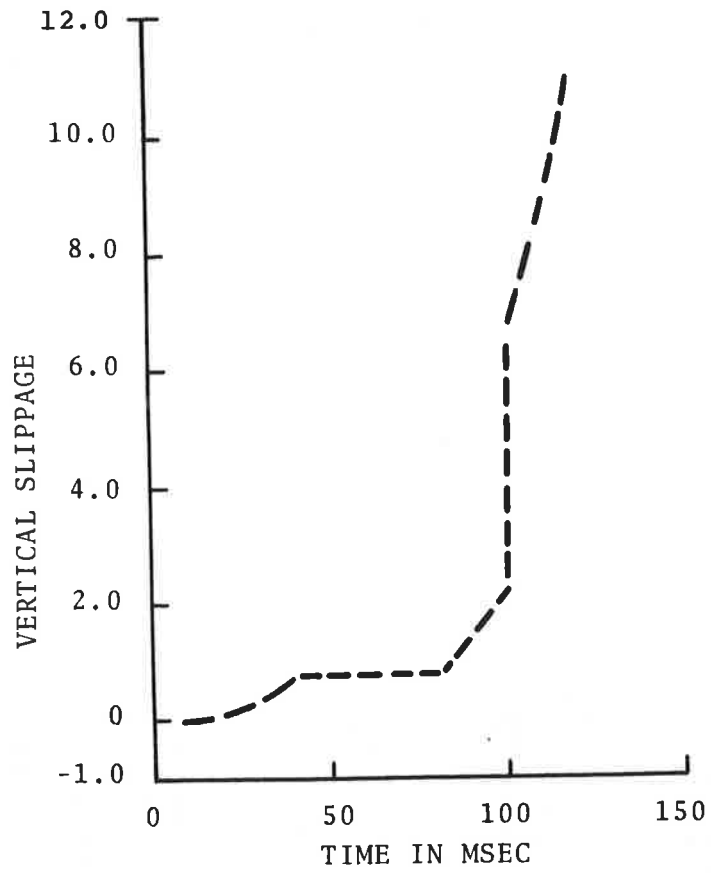


FIGURE 15. SLIPPAGE BETWEEN THE IMPACTED CAR AND THE BACK UP CAR FOR 18.1 MPH IMPACT

TABLE 3. MATERIAL PROPERTIES OF BEAM ELEMENTS OF CABOOSE

Element #	Area (in <sup>2</sup> )	Young's Modulus (psi)	Rotary Inertia (in <sup>4</sup> -lb)	Mo (in-lb)	Fyo (lbs)
1,2	22.4	16. x 10 <sup>6</sup>	596.5	3.36 x 10 <sup>6</sup>	.6 x 10 <sup>6</sup>
3,4	5.	30. x 10 <sup>6</sup>	200.	3.36 x 10 <sup>6</sup>	.6 x 10 <sup>6</sup>
5,7	5.	16. x 10 <sup>6</sup>	400.	3.36 x 10 <sup>6</sup>	.3 x 10 <sup>6</sup>
6	1.5	16. x 10 <sup>6</sup>	10.	.166 x 10 <sup>6</sup>	.1 x 10 <sup>6</sup>
8,9	1.	16. x 10 <sup>6</sup>	1.5	3.36 x 10 <sup>6</sup>	.3 x 10 <sup>6</sup>

TABLE 4. WEIGHT AND ROTARY INERTIA OF EACH NODE OF CABOOSE

Node #	Weight (lbs)	Rotary Inertia (lb-in-sec <sup>2</sup> )
1,5	6,000.	12,000.
2,4,6	2,300.	10,000.
3	9,120.	10,000.

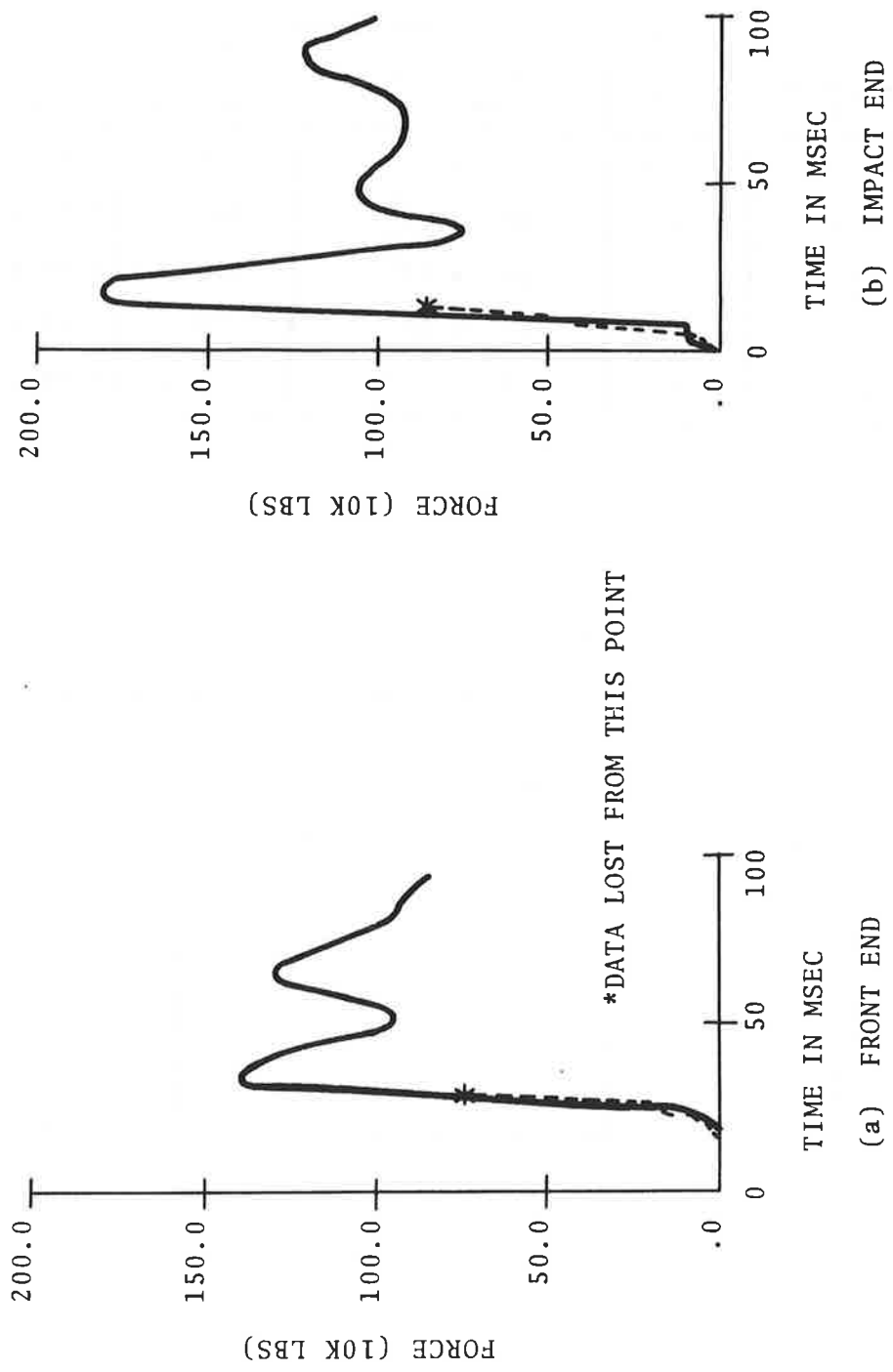


FIGURE 16. LONGITUDINAL FORCES ON THE CABOOSE FOR A 30.3 MPH IMPACT —  
 COMPUTER SIMULATION --- FULL SCALE TEST

## 5. CONCLUSIONS, DISCUSSIONS AND RECOMMENDATIONS

Both simple and comprehensive mathematical models have been developed to simulate the motion and the deformation of trains in collision. Results of the analytical investigation and those of the two full scale train-train impact tests are in reasonably good agreement. However, the predictive capability of the analytical model still depends critically on good input parameters. These parameters include the weight, the mass moment of inertia of cars and loadings, the length of cars, the location of the center of gravity, the longitudinal, the vertical and the lateral stiffness and strength, the alignment and the slack between cars, the draft gear capacity, etc.

This study has given insight toward understanding many of the causes and the consequences of train motions in impact. The next question now is how the understanding can be utilized to resolve some of the problem arising from collision. There is usually an enormous amount of kinetic energy in a moving train. The dissipation of this energy in order to eliminate or at least to reduce the loss of lives and the damage of properties in a train collision is an important problem. The normal mechanism of dissipating energy is through the brakes of the draft gears. The other way is to properly control the transfer of a part of the kinetic energy from the moving train to the standing one in a non-destructive or in a minimally destructive manner. The first two mechanisms are often insufficient to dissipate enough energy in a short time, especially in the case of a high speed collision (say about 10 mph). Dissipation of the kinetic energy in a controlled manner seems to be the critical factor in minimizing the losses in an accident.

The most devastating result of a train collision occurs when some of the cars overrides the others, intruding into the superstructure of the overridden cars and killing their passengers. Questions dealing with the causes of override and circumstances leading to them, have been examined carefully. In the following,

we shall summarize the results and make recommendations on the control of kinetic energy dissipation:

A rail car is usually heavy and large longitudinal forces will be generated in collision. These forces can be estimated by a simple one dimensional spring-mass system (e.g., Figure 2). In the cases of the impact of two cars and the impact of a heavy car onto a light car backed up by a heavy car (or cars), the maximum forces were estimated in Eqs (1) and (2) respectively.\* The maxima are proportional to the impact speed and the square root of the effective mass [e.g.,  $m_1 m_2 / (m_1 + m_2)$  in the case of two car impact] and the stiffness between cars. This is generally true for impact involving many cars. In other words, the total mass of a train has little effect on the magnitude of the longitudinal forces developed. Therefore, in order to minimize losses in accidents, we can deal with the individual car only in controlling the magnitude of the forces and its points of application. This is so because it is the large force that is responsible for structural failure, even though the extent of the failure and damage depends predominantly on the total kinetic energy present. We shall discuss the control of load application later. To control the force magnitude, we can reduce the impact speed, the longitudinal stiffness or the mass of each individual car, or limit the strength of some components such as the draft gears.

From Section 2, we see that the force magnitude can exceed a million pounds for an impact above 10 mph. Under this circumstance, braking will only have little effect\*\* on the drastic change of vehicle motion in the short time during impact. However, braking on the moving train, especially for a consist made up of heavy cars and followed by light cars and no braking on the stationary train will help to reduce the build up of forces.

---

\*The result is based on an elastic analysis. The actual maximum value is limited by the yielding strength of the coupler, the draft gear or the center sill.

\*\*For a car weighing 50,000 lbs and a friction coefficient of 0.1, the friction force is about 5,000 lbs.

For most of the rail cars, the longitudinal stiffnesses are concentrated on the floor level. This is particularly true for a freight car where the center sill carries the majority of the longitudinal force. The coupler face is the only place transmitting this load and is only about 11 inches in height. A vertical mismatch of the two cars in collision by this amount will result in an override and can cause extensive damage to the overridden car. Such a mismatch can just be the initial misalignment in the coupler height before impact and/or be the induced misalignment during impact.

The induced mismatch is the result of the pitching and the vertical motions which are primarily caused by the longitudinal forces, not acting through the center of gravity of a car, and not being parallel to the horizontal direction. Since the longitudinal force is large, it can create a large pitching motion even if the moment arm about the center of gravity is small. It can also cause large vertical and pitching motion if it acts at a small angle to the horizontal direction. The moment arm in the vertical direction is approximately the distance between the center line of the coupler to the c.g. height.\* Since the coupler is generally lower than the center of gravity, an impact between two cars usually causes the impact end to pitch down (at least initially). The orientation of the longitudinal force is affected mainly by the misalignment both prior to and during an impact, and by the deformation of the components such as the coupler shank, the draft gear and the center sill. The combination of bending and compression can change the vertical force significantly by causing a large rotation of these components when the yield strength of these components is reached. This is because the structural steel usually has little strain hardening, and can be bent easily (like a hinge) when yielding occurs.

From these discussions, it seems that the key to control override is to control the misalignment and the vertical motion. The initial misalignment of the coupler heights can be minimized

\*It is about 2 ft. for a caboose and about zero for a light flat car.

by proper maintenance and inspection in operation. The induced misalignment in impact can be reduced by restraining the vertical motion. There are two situations: (1) when a light car is impacted, it can bounce up easily to override the other car, especially when there is no back up car or the back up car is separated by some distance of order a foot or more (see Section 4.2 and 4.3). This can happen in a switch yard, because cars humped above 6 mph often do not couple\* causing several feet separation from the rest of the train. In order to improve such situation, one should make sure that cars are coupled in humping operation by some inspecting procedures and by improving the coupling mechanism such as making it easier for the coupler pin to drop. (2) when a heavy car is impacted by another heavy car, normally there will be less induced vertical and pitching motion than the case in which a light car is involved. However, the longitudinal force will be large (see equation 1), and it can easily exceed the yielding strength of the components. The resulting local buckling or plastic deformation of the coupler or the center sill will cause a large rotation of these components which can make the couplers of the two impacting cars slip off from each other.\*\* This situation can also happen in the impact of light car at higher speed (approximately above 20 mph) or of a heavy car on a light car backed up by a heavy car or cars. To improve this situation, it is recommended that: (a) increase the yielding strength of the coupler and the center sill (which can include improving structural design to utilize to maximum extent the strength of the side walls, the roof and the floor); (b) increase the vehicle stiffness in vertical direction for both bending and translation, such that in the event of buckling and the formation

---

\* It is particularly true in the humping of light cars, because the contact time between two cars is shorter for the impact of light cars than that of heavy cars, therefore there is less chance for the coupler pin to drop to lock the coupler.

\*\* For a standard E-coupler, there is no constraints in the vertical direction between two couplers besides the friction forces between the coupler faces when the knuckles are pressed against each other.

of plastic hinge the rotation of the coupler and/or the center sill will be more in the lateral direction than in the vertical direction which would cause the car to move laterally rather than vertically, (c) add vertical restraints so that the couplers cannot slip off each other vertically; and (d) increase the capacity of the draft gear to dissipate more kinetic energy and to limit (or at least to reduce) the magnitude of the longitudinal force.

The main idea in the above suggestions is to limit the vertical motion of a car and to confine the slippage of the couplers so that the stiff parts of two cars will remain in contact. This will aid the kinetic energy transfer and dissipation during impact. However, in a high speed collision, the coupler or the center sill can be broken\* and will no longer provide any vertical restraints, or damaged severely causing the entire car to buckle (Figure 1.5) and to be pushed up onto another car as seen in the 30.3 mph locomotive caboose test (Figure 17). Thus the superstructure of a car must still be protected, especially for cars such as locomotives or passenger cars or for cars carrying hazardous materials. However, it is impractical economically for the protection of the superstructure by designing a structure which can withstand the impact at 20 or 30 mph by another car of weighing 50,000-100,000 lbs. The solution seems to be to make the structure strong enough with a contour which will deflect an impacting car rather than absorb the impacting kinetic energy.

Some of the various ideas of improving the crashworthiness and reducing the tendency to override for rail cars is summarized schematically in Figure 18. In Figure 18 a locomotive is shown with the following features: a modified coupler where the stiffness and strength in the vertical direction are higher than those in the lateral direction; an anticlimber over the top of its coupler to prevent the coupler of another car moving up to override the locomotive; and a sloping thick shell structure in front of the

---

\*Especially in cold weather where the metal becomes very brittle.



FIGURE 17. FINAL CONFIGURATION OF THE CABOOSE AFTER THE 30MPH COLLISION

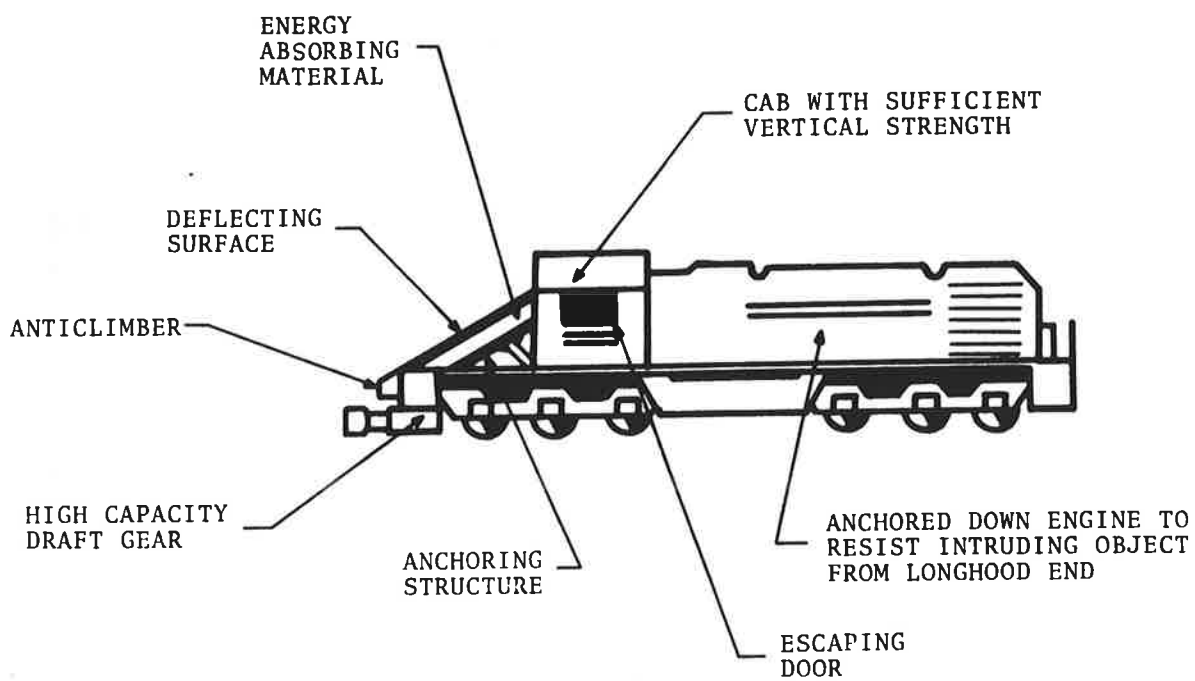


FIGURE 18. CRASHWORTHY AND OVERRIDEWORTHY LOCOMOTIVE

cab at the short end to deflect an intruding object vertically and/or laterally. The structures at the longhood end are anchored properly to the sills to protect this end against intrusion.

The actual design of these fixtures and of the tests to verify their effectiveness are still in planning stage and are the subject of a future report.

APPENDIX A  
LONGITUDINAL AND VERTICAL MOTION OF  
THREE IMPACTING MASSES

The equations for the longitudinal motion of the three impacting masses shown in Figure 2 are

$$\begin{aligned} m_1 \ddot{x}_1 + k_1(x_1 - x_2) &= 0 \\ m_2 \ddot{x}_2 + k_1(x_2 - x_1) &= 0 \\ \ddot{x}_3 &= 0 \end{aligned} \tag{A.1}$$

before the slack between  $m_2$  and  $m_3$  is taken up, i.e.,  $x_2 \leq \delta$  and  $t \leq t_0$ , and

$$\begin{aligned} m_1 \ddot{x}_1 + k_1(x_1 - x_2) &= 0 \\ m_2 \ddot{x}_2 + k_1(x_2 - x_1) + k_2(x_2 - x_3 - \delta) &= 0 \\ m_3 \ddot{x}_3 + k_2(x_3 - x_2 + \delta) &= 0 \end{aligned} \tag{A.2}$$

for  $t > t_0$ .

The solution of Eq. (A.1) is simply

$$\begin{aligned} x_2 - x_1 &= -\frac{V}{\omega_0} \sin \omega_0 t \\ x_2 &= \frac{V m_1}{m_1 + m_2} \left( t - \frac{\sin \omega_0 t}{\omega_0} \right) \end{aligned} \tag{A.3}$$

for  $x_2 \leq \delta$ , where

$$\begin{aligned} \omega_0 &= \sqrt{\frac{k_1}{m}} \\ m &= \frac{m_1 m_2}{m_1 + m_2} \end{aligned}$$

the quantity  $m$  is usually called the equivalent mass for the impact of two bodies. Note that  $t_0$  can be evaluated from Eq. (A.3), i.e.,

$$\delta = \frac{V m_1}{m_1 + m_2} \left( t_0 - \frac{\sin \omega_0 t_0}{\omega_0} \right) \quad (\text{A.4})$$

The longitudinal forces on both ends of the impacted car are

$$\begin{aligned} F_1(t) &= k_1(x_1 - x_2) = V\sqrt{k_1 m} \sin \omega_0 t \\ F_2(t) &= 0 \end{aligned} \quad (\text{A.5})$$

for  $0 < t \leq t_0$ .

The solution of Eq. (A.2) can be obtained straightforwardly for  $t \leq t_0$ , but it is somewhat lengthy. We shall only consider a special case where  $m_2$  is light, i.e.,  $m_1 \gg m_2$ , the freight car is loaded, i.e.,  $m_3 \gg m_2$  and  $\delta$  is sufficiently small, such that  $\delta < V m_1 \pi / (m_1 + m_2) \omega_0$ . Using these facts, one can easily construct an approximate solution of Eq. (A.2). From the approximate solution for  $t > t_0$ , we have the longitudinal forces

$$\begin{aligned} F_1(t) &= k_1(x_2 - x_1) \\ &\approx + V \sqrt{\frac{k_1 k_2}{k_1 + k_2} \frac{m_1 m_3}{m_1 + m_3}} \sin(\Omega t + \psi) + \frac{V}{2} \sqrt{\frac{k_1^2 m_2}{k_1 + k_2}} \rho \sin(\omega t + \phi) \\ F_2(t) &= k_2(x_3 - x_2 + \delta) \\ &= V \sqrt{\frac{k_1 k_2}{k_1 + k_2} \frac{m_1 m_3}{m_1 + m_3}} \sin(\Omega t + \psi) - \frac{V}{2} \sqrt{\frac{k_2^2 m_2}{k_1 + k_2}} \rho \sin(\omega t + \phi) \end{aligned} \quad (\text{A.6})$$

where

$$\tau = t - t_0$$

$$\Omega^2 = \frac{k_1 k_2}{k_1 + k_2} \frac{m_1 + m_3}{m_1 m_3} \left[ 1 - \frac{(k_1 m_1 - k_1 m_3)^2 m_2}{(k_1 + k_2)^2 m_1 m_3 (m_1 + m_3)} \right]$$

$$\begin{aligned}
\omega^2 &= \frac{k_1+k_2}{m_2} \left[ 1 + \frac{m_2}{(k_1+k_2)^2} \left( \frac{k_1^2}{m_1} + \frac{k_2^2}{m_3} \right) \right] \\
\rho &= (\alpha^2+\beta^2)^{1/2} \\
\alpha &= \frac{2k_2}{k_1+k_2} - 2 \cos \omega_0 t_0 \\
\beta &= - 2 \sqrt{\frac{k_1}{k_1+k_2}} \sin \omega_0 t_0 \\
\phi &= \tan^{-1} \beta/\alpha \\
\psi &= \tan^{-1} \left( \frac{\Omega}{\omega_0} \sin \omega_0 t_0 \right)
\end{aligned} \tag{A.7}$$

In evaluating the forces, the information on the masses is generally available. The value of the stiffness must be measured or be estimated by

$$\begin{aligned}
2 k_1 &= f E \left/ \left( \frac{L_2}{A_2} + \frac{L_1}{A_1} \right) \right. \\
2 k_2 &= f E \left/ \left( \frac{L_2}{A_2} + \frac{L_3}{A_3} \right) \right.
\end{aligned} \tag{A.8}$$

where E is the Young's modulus, A is the cross section area and L is the half length of the center sill subscripts 1, 2, and 3, denote the impacting car, the impacted car and the back up car respectively. The quantity, f, is a dynamic correction factor which can be greater or less than one. Usually when the structure experiences instability such as local buckling and crushing, etc. f can be larger than one. Otherwise it is typically less than one. This is because most of the mass of the structure is not rigidly attached to the center sill which makes the effective stiffness smaller. From the data of the full scale impact tests, f is estimated to be between 1/3 and 1/5.

The longitudinal forces are usually below the center of gravity (Fig. 4), so that pitch and vertical motions are induced. The approximate equations of motion are \*

$$\begin{aligned} m_2 \ddot{v} + k_t(v - \ell\theta) + (k_t + k_v)(v + \ell\theta) &= eF_1(t) \\ I_2 \ddot{\theta} + k_t\ell(\ell\theta - v) + (k_t + k_v)\ell(v + \ell\theta) &= -hF_1(t) + eL F_1(t) \end{aligned} \quad (\text{A.9})$$

for  $t \leq t_0$ , where  $m_2$  and  $I_2$  are the impacted car mass and rotary inertia respectively,  $k_t$  is the spring constant of one truck, and  $k_v$  is the vertical spring constant of the center sill. The term  $eF_1(t)$  is introduced to account for the misalignment of the couplers with  $e$  being the angle of the resultant forces. The exact direction of the longitudinal forces depends on the relative height of the couplers between the two impacting cars, the shape and the deformation of the impacting surface, etc. As a first order approximation, we assume that\*\*

$$e = \frac{\text{difference of the coupler heights}}{\text{distance of the draft gears between the two cars}} \quad (\text{A.10})$$

In practice  $k_t \ll k_v$ . For example the value of  $k_t$  for a caboose is of the order of 9000 lb/in and  $k_v$  is usually greater than 50,000 lb in (after the draft gear has bottomed out). Using equation (A.1) for  $F_1(t)$ , we may approximate (A.9) as follows:

$$\begin{aligned} m_2 \ddot{v} + (k_t + k_v)(v + \ell\theta) &= e V\sqrt{k_1 m} \sin \omega_0 t \\ I_2 \ddot{\theta} + (k_t + k_v)\ell(v + \ell\theta) &= - (h - eL) V\sqrt{k_1 m} \sin \omega_0 t \end{aligned} \quad (\text{A.11})$$

where  $m$  and  $\omega_0 = \sqrt{k_1/m}$  are defined in (A.3). This approximation is equivalent to assume the motion being pivoted at the impact end truck. Its solution is

\* Since  $t_0$  is small, and  $F_1$  is much larger than the gravitational force, therefore the gravitational force can be neglected for  $0 \leq t \leq t_0$ .

\*\* This is equivalent to assuming that the couplers are pivoted at the draft gears.

$$v + \ell\theta = A \omega_0 \frac{\frac{\omega_v t}{\omega_v} \sin \omega_v t - \sin \omega_0 t}{\omega_v^2 - \omega_0^2}$$

$$v = \frac{k_t + k_v}{m_2} A \left[ \left( \frac{\omega_0}{\omega_v} \frac{\sin \omega_v t}{\omega_v^2} - \frac{\sin \omega_0 t}{\omega_0^2} \right) \frac{\omega_0}{\omega_v^2 - \omega_0^2} - \frac{t}{\omega_v^2} \right] \quad (\text{A.12})$$

where

$$\omega_v = \frac{k_t + k_v}{I_2} \left( 1 + \frac{\ell^2 m_2}{I_2} \right)$$

$$\Lambda = \frac{V m}{I_2} \left[ \ell h - e \left( \frac{I_2}{m_2} + \ell L \right) \right] \quad (\text{A.13})$$

The two cars separate from each other at  $t = \pi/\omega_0$ . After separation, the motion of  $m_2$  involves only the interaction of the car body and its trucks. If there is little or no misalignment,  $A > 0$  in Eq. (A.13) and the impact end pitches down during impact. At the time of separation, the car body is likely to lift up from the front truck. The truck at the impact end will be the only pivot point for the car body. The equations of motion are

$$m_2 \ddot{v} + k_t (v + \ell\theta) = -m_2 g$$

$$I_2 \ddot{\theta} + k_t \ell (v + \ell\theta) = 0 \quad (\text{A.14})$$

which are similar to equation (A.11) except for the right hand sides. The solution is

$$v + \theta l = - \frac{g}{\omega_t^2} \left( 1 - \cos \omega_t \tau + (v_o + l \dot{\theta}_o) \right) \cos \omega_t \tau + \frac{(\dot{v}_o + \dot{\theta}_o l)}{\omega_t} \sin \omega_t \tau$$

$$v = \frac{1}{1 + \frac{l^2 m_2}{I_2}} \left[ \left( - \frac{m_2 l^2}{I_2} + \frac{\cos \omega_t \tau - 1}{\omega_t^2} \right) g + (v_o + l \dot{\theta}_o) \cos \omega_t \tau \right. \\ \left. + (\dot{v}_o + l \dot{\theta}_o) \left( \frac{\sin \omega_t \tau}{\omega_t} - 1 \right) \right] + \dot{v}_o \tau + v_o$$

where

$$\tau = t - \pi/\omega_o$$

$$\omega_t = \sqrt{k_t/m_2} \quad (A.15)$$

To compute the maximum height of the impacted car we should consider two extreme cases: Case a. we assume  $\omega_v \gg \omega_o$ ,  $\omega_t$  (rad/sec)  $\gg 1$  and  $e=0$ . For  $t > t_o$ , we have

$$v + l \theta = 0$$

$$v = - \frac{1}{2} \frac{m_2 l^2 g}{I_2 + l^2 m_2} \left( t - \frac{\pi}{\omega_o} \right)^2 + \dot{v}_o \left( t - \frac{\pi}{\omega_o} \right) + v_o \quad (A.16)$$

where  $v$  is the vertical displacement of the center of gravity the maximum displacement is given in Eq. (10).

Case b, we assume that  $\omega_v \ll \omega_o$  and  $\omega_t$  (rad/sec)  $\ll 1$ . This is to say that during impact, the pitch down motion of the caboose at the impact end has caused the truck springs to bottom out. Therefore the truck becomes very stiff in the vertical direction ( $k_t$  large). From Eqs. (6) and (7), we have

$$v_o + \theta_o \ell = - \frac{\ell h V m}{I_2} \frac{\pi}{\omega_o}$$

$$v_o = 0 \quad (A.17)$$

and

$$\dot{v}_o + \dot{\theta} \ell = - \frac{2 \ell h V m}{I_2}$$

$$\dot{v}_o = 0 \quad (A.18)$$

At  $t - \pi/\omega_o = \pi/\omega_t$ , from (A.12), the vertical velocity is

$$\dot{v} + \dot{\theta} \ell = \frac{2 \ell h V m}{I_2}$$

$$\dot{v} = \frac{4 \ell h V m}{I_2 + m_2 \ell^2} \quad (A.19)$$

and

$$v + \theta \ell = - \frac{\ell h V m}{I_2} \frac{\pi}{\omega_o}$$

$$v = 0 \quad (A.20)$$

(The approximation  $\omega_t$  (rad/sec)  $\gg 1$  has been used.) At this time, the car body lifts off the truck at the impact end and moves upward. The vertical velocity of the coupler is then

$$\dot{v}_I = \dot{v} + \dot{\theta} L = \frac{2 h V m}{I_2 + m_2 \ell^2} \left[ 2 \ell + L \left( \frac{m_2 \ell^2}{I_2} - 1 \right) \right]$$

and its vertical displacement is

$$v_I = - \frac{1}{2} g \left( t - \frac{\pi}{\omega_o} - \frac{\pi}{\omega_t} \right)^2$$

$$+ \dot{v}_I \left( t - \frac{\pi}{\omega_o} - \frac{\pi}{\omega_t} \right) - \frac{L h V m}{I_2} \frac{\pi}{\omega_o} \quad (A.21)$$

The maximum value of  $v_I$  is reached at

$$t = \frac{\pi}{\omega_o} + \frac{\pi}{\omega_t} + \frac{\dot{v}_I}{g}$$

with a value of

$$(v_I)_{\max} = \frac{1}{2} \frac{\dot{v}_I^2}{g} - \frac{LhVm}{I_2} \frac{\pi}{\omega_o} \quad (\text{A.22})$$

Using the parameters considered in case a, we have

$$\dot{v}_I = 1.39 \text{ in./sec.}$$

and at

$$t = 0.048 + 0.36 = 0.4 \text{ secs.}$$

The maximum coupler height at the impact end is

$$(v_I)_{\max} = 21 \text{ in.} \quad (\text{A.23})$$

Comparing the results, e.g., Eqs. (15) and (A.23), of the two extreme cases of different vertical stiffness, it is clear that the induced vertical motions are drastically different. In case a, the front end pitches up higher than the impact end while in case b, the impact end moves up higher.

## APPENDIX B

### MODELING OF TRAINS BY FINITE ELEMENT MODULES

References 3 and 4 model the two dimensional motion of a rail car (including the trucks) as a single rigid body. A vertical and a horizontal massless springs are used to simulate the deformation of the draft gear and the center sill, and a massless vertical spring is used to represent the deformation of the truck.

The present analysis uses the modular approach of the finite element method.<sup>5</sup> This approach enables the modeling of the various cars of a train and the various parts of a car with different degrees of detail. The differences from that of references 3 and 4 are then, in the present model, (1) the car body and the trucks are modeled separately, which are connected by a vertical and a horizontal spring. This is because, in reality, the trucks do move relatively to the car body in both the vertical and the horizontal direction. Its masses are not small as compared to that of the car body (especially for a light car such as a caboose, two trucks weigh about 7000 lbs each and the car body weighs about 28,000 lbs). (2) The bending of the sill and the draft gear are included to account for the restraint on the pitching motion of the cars. Because under a high compressive force, the coupler and the sill act as a unit and give a large restraint to the relative pitching of the two impacting cars. (3) There are two ways in modeling of car body. Usually, it is modeled as a rigid body. However, in the case of an high speed impact, some of the car bodies can experience large deformation. For those cars, a refinement in modeling to simulate the body deformation is shown in Figure 11 where the structure of the car body is represented by deformable beams with the mass and the rotary inertia distributed at all the nodes.

All springs are assumed to have force deflection characteristics as shown in Figure 19, in which the yielding force,  $F_y$ , can be the function of strain rates.

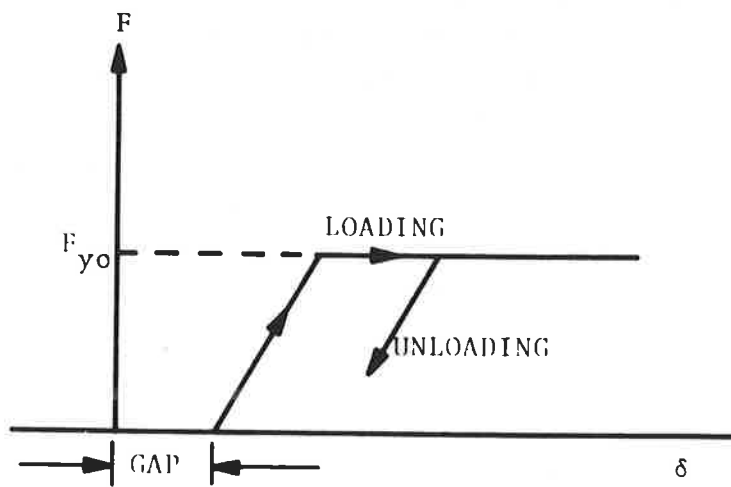


FIGURE 19. TYPICAL SPRING CHARACTERISTICS

$$F_y = F_{y0} \left( \frac{\alpha \dot{e} + 1}{\beta \dot{e} + 1} \right)^n \quad (\text{B.1})$$

where

$$\alpha \geq \beta \geq 0, n > 0,$$

$F_{y0}$  are the static yield strength. The track, the truck, the bolster, and the underframe spring will take compression load only. The draft gears between two cars will take both compression and tension, if engaged, and only compression if disengaged. In practice, the truck in the horizontal direction, the bolsters, the underframe and the track, are much stiffer than the draft gear and the truck spring in vertical direction.

A list of the values of these quantities for a locomotive, a caboose and a hopper car is given in Table 2.

The beam element used for those car body involving large deformation and for the underframe are developed by Tong is reference 5. The beams are allowed to have large displacement and rotation and to have plastic hinge at the end nodes of each element. The yielding surface for the plastic hinge is:

$$\phi = \left( \frac{M}{M_0} \right)^2 + \left( \frac{F}{F_{y0}} \right)^2 - \left( \frac{\alpha \dot{e} + 1}{\beta \dot{e} + 1} \right)^{2n} = 0 \quad (\text{B.2})$$

where  $M$  and  $F$  are the moment and the longitudinal force, and  $M_0$  and  $F_{y0}$  are constants which are respectively the yield moment and the yield strength in the longitudinal direction.

There are some special considerations for underframe beam element to account for induced vertical force due to slippage between the coupler and for the horizontal truck spring element to account the tilt of the truck bolster. We shall discuss them separately.

### Underframe Beam Element

The longitudinal forces generated by the draft gear and the underframe are not always parallel to the ground. Its vertical components are computed as follows: In Figure 20,  $s$  denotes the offset of two impacting couplers,  $v_1$  and  $v_2$  are the end vertical displacements of the two impacting cars,  $d$  is the distance between two draft gears, the dotted lines indicate the deformation and the arrows show the direction of positive sign of the corresponding quantities. The angle between the longitudinal force and the horizontal direction is:

$$e = \frac{v_2 - v_1 - s}{d} + 1.5 \frac{s}{d} \quad (\text{B.3})$$

The first term is to account for the directional change of the longitudinal force due to the relative end displacement of the two cars and the second term is to account the induced vertical force due to an offset,  $s$ , of the neutral axis of a beam. Thus the induced vertical force is  $eF$ . It should be noted that the offset  $s$ , also induced moments of  $\frac{1}{4} sF$  at both ends.

Between two E-couplers, friction is the only restraint in the vertical direction. When the force parallels the coupler face exceeds the friction force, slippage between two couplers occurs. The angle between the coupler face and the vertical line is computed from the beam theory,

$$\theta = \frac{3}{2} \frac{v_2 - v_1 - s}{d} - \frac{\theta_2 + \theta_1}{4} + \frac{Fs\ell}{4EI} \quad (\text{B.4})$$

where  $\theta_2$  and  $\theta_1$  are the rotation of the two impacting cars. The first two terms in Eq. (B.4) are due to the motion at the ends and the last term is induced by the compression force,  $F$ , with an offset,  $s$ . We assume the friction force to be  $\mu F$ .

There are two cases: (a)  $\mu - |\theta| > 0$ , if

$$|F_v| \leq (\mu - |\theta|) |F| \quad (\text{B.5})$$

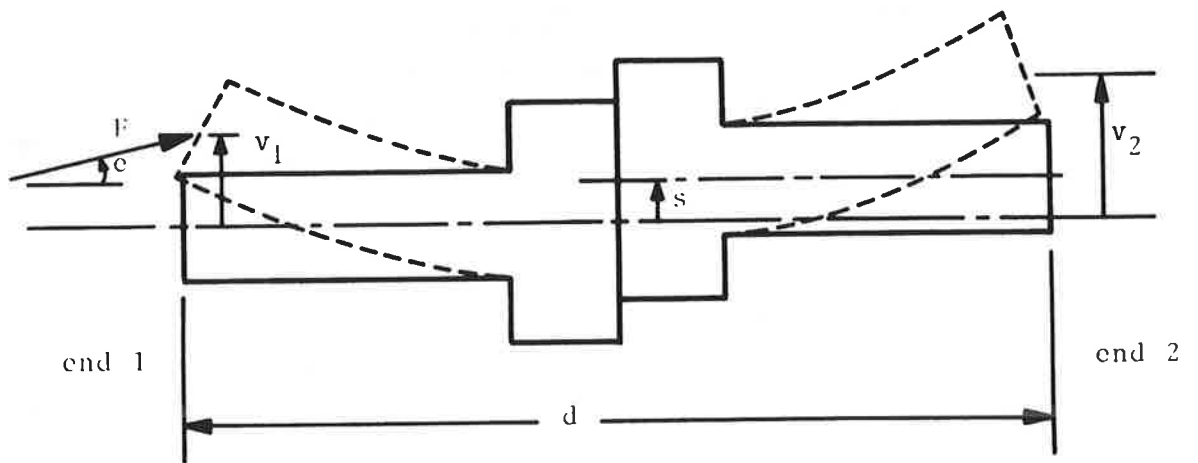


FIGURE 20. TWO IMPACTIVE COUPLERS WITH DOTTED LINES INDICATE THE DEFORMATION

in which  $F_v$  is the force component parallel to the coupler faces, then there will be no slippage between couplers. Otherwise slippage occurs such that

$$|F_v| = (\mu - |\theta|) |F| \quad (B.6)$$

(b)  $\mu - |\theta| \leq 0$ . The two couplers are free to slide relative to each other. In this case both  $F$  and  $F_v$  reduce to zero. And offset of the two couplers becomes

$$s = v_2 - v_1 - \frac{d}{2} (\theta_2 + \theta_1) \quad (B.7)$$

#### Horizontal Truck Spring Element

When the car body move horizontally relative to the truck, it is assumed that the truck bolster will tilt and the body center plate will slip out from the bowl of the truck if

$$|F_h|d_1 > |F_t|d_2$$

where  $d_1$  is the vertical distance from the top of the rim of truck bowl to the middle of the truck bolster and  $d_2$  is sum of the center plate radius and a quarter of the width of the truck bolster,  $F_h$  and  $F_t$  are respectively the horizontal and the vertical force acting on the truck by the car body. When the center plate slips out from the bowl,  $F_h$  will become zero.

#### Numerical Problems

The approximation of the car bodies as rigid elements is essential in the saving of computing time. If the car bodies are modeled as deformable bodies, the highest natural frequency of the finite element system (which can be estimated in a straightforward manner, reference 6 ) can be much higher than that of the system modeled with rigid elements. In using the explicit scheme for numerical integration, the numerical stability approximately requires the time increment, such that\*

\*This requirement is exact for a linear system.

$$\Delta t < \frac{2}{\omega_{\max}}$$

where  $\omega_{\max}$  is the highest natural frequency in radian/sec. If the time increment requirement decreases, the computer time will have to increase accordingly because it will take more time steps to simulate a given length of real time and the simulation of the deformable body will require more computer time for each time step.

There is another restraint in the allowable time increment involving plastic deformation. After the structure yields, plasticity theory requires the stress field remain on the yielding surface for loading situation. However, the flow rule of the incremental plasticity theory is based on the assumption of infinitesimal loading increment. In practice, the finite time step size in numerical computation results in a finite increment in stress field. If the step size is too big, the incremental stress cannot remain on the yield surface (the solution of equation (3.17) of reference 5 becomes imaginary). This is illustrated in the schematic diagram shown in Figure 21.  $\underline{\sigma}_0$  is the stress state of the previous step.  $d\underline{\sigma}_t$  is the total stress increment of the present time step if the deformation is elastic.  $d\underline{\sigma}_p$  is the stress correction due to plastic deformation and

$$d\underline{\sigma} = d\underline{\sigma}_t - d\underline{\sigma}_p$$

is the actual stress increment such that

$$\underline{\sigma} + d\underline{\sigma}$$

should lie on the yield surface. As shown in Figure 21, if  $d\underline{\sigma}_t$  is too big, a parallel line of  $d\underline{\sigma}_p$  from  $d\underline{\sigma}_t$  will not intersect with the yield surface. Such a limitation can be identified as the accuracy requirement in the plasticity computation.

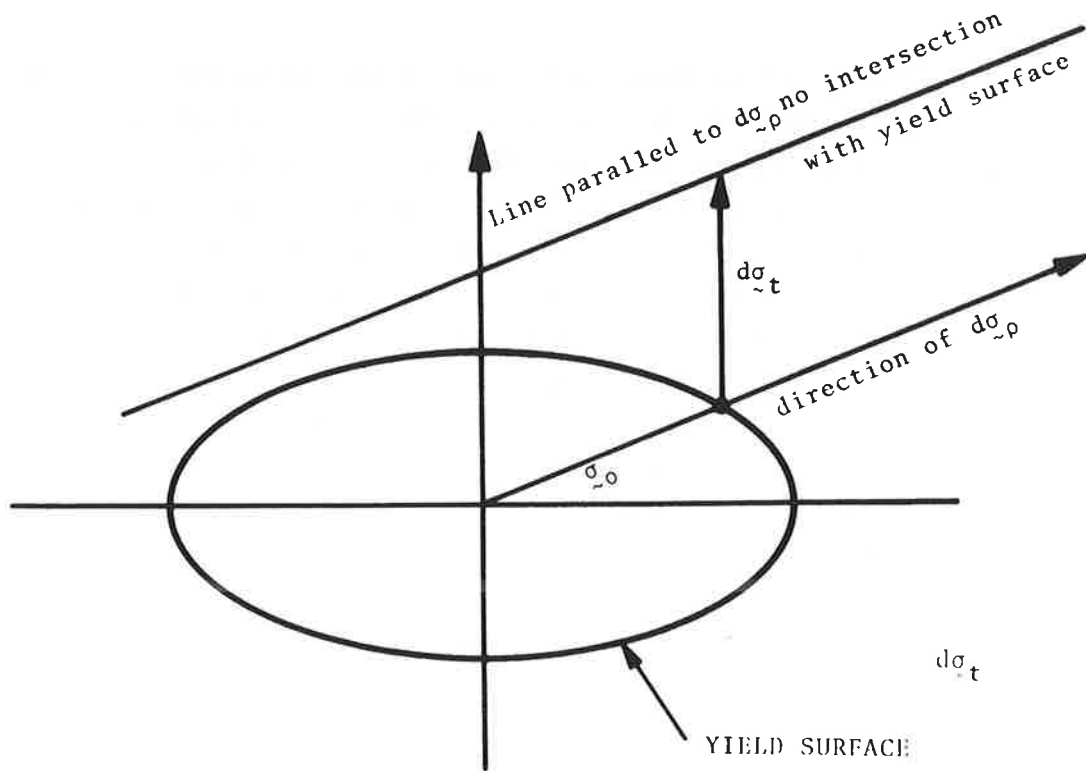


FIGURE 21. SCHEMATIC DIAGRAM OF THE FAILURE OF APPROXIMATE SOLUTION IN ELASTIC PLASTIC ANALYSIS

## REFERENCES

1. FRA Accident Bulletin No. 135 to No. 143 (1966-1974) "Summary and Analysis of Accidents on Railroads in the United States," 1975.
2. Hawthorne, K.L., "A Preliminary Study of Head-on and Rear-end Collision Involving Locomotive," V-804-74-01, Research and Test Dept., Assoc. of American Railroads, 1974.
3. Raidt, J.B., "A Preliminary of Vertical Motions During Impact," Pullman Standard Research Proj. No. 39-1853, August, 1972.
4. Hohenemser, K.H., Diboll, W.B., Yin, S.D. and Szabo, B., "Computer Simulation of Tank Car Head Puncture Mechanism," Report No. FRA-ORD&D-75-23, Feb. 1975.
5. Tong, P. and Rossettos, J., "Modular Approach to Structural Simulation for Vehicle Crashworthiness Prediction," Rpt. No. DOT-TSC-NHTSA-74-7, March 1975.
6. Tong, P., "On the Numerical Problems by the Finite Element Methods," Computer Aided Engineering Edited by Gladwell, Univ. of Waterloo, Waterloo, Canada, pp 539-560, 1974.
7. Cramer, P.L. and Anderson R.L., "Train-to-Train Impact Tests," Vol. I and II, Dynamic Science Rept. No. 8261-75-155, DOT-TSC-840, 1975.

